Mechanistic Analysis of the Broad Antiretroviral Resistance Conferred by HIV-1 Envelope Glycoprotein Mutations

Short title: Broad resistance to antiretrovirals mediated by HIV-1 Env

Yuta Hikichi[1], Rachel Van Duyne[1, #a], Phuong Pham[1], Jennifer L. Groebner[2], Ann Wiegand[2], John W. Mellors[3], Mary F. Kearney[2], Eric O. Freed[1*]

[1] Virus-Cell Interaction Section, HIV Dynamics and Replication Program, NCI-Frederick, Frederick, Maryland, United States of America

[2] Translational Research Section, HIV Dynamics and Replication Program, NCI-Frederick, Frederick, Maryland, United States of America

[3] Department of Immunology, University of Pittsburgh, Pittsburgh, Pennsylvania, United States of America

[#a] Current Address: Department of Pharmacology and Physiology, College of Medicine, Drexel University, Philadelphia, Pennsylvania, United States of America

* Corresponding author

E-mail: efreed@mail.nih.gov (EOF)

Abstract

Despite the effectiveness of antiretroviral (ARV) therapy, virological failure can occur in some HIV-1 infected patients in the absence of mutations in the proteins targeted by these drugs. We previously reported that, *in vitro*, the lab-adapted NL4-3 strain of HIV-1 can acquire resistance to the integrase inhibitor dolutegravir (DTG) by acquiring mutations in the envelope glycoprotein (Env) that enhance the ability of HIV-1 to spread via cell-cell transmission. In this study, we investigated whether Env-mediated drug resistance extends to ARVs other than DTG and whether it occurs in other HIV-1 isolates. We demonstrate that Env mutations can broadly confer resistance to multiple classes of ARVs in the context of cell-cell but not cell-free infection and also increase resistance to ARVs when coupled with target-gene drug resistance mutations. To investigate the mechanism of Env-mediated drug resistance, we evaluated the impact of the Env mutations on Env stability and conformational dynamics. We observe that the NL4-3 Env mutants display a more stable and closed Env conformation compared to WT virus and reduced rates of gp120 shedding. We also selected for mutations in the gp41 ectodomain of clinically relevant, CCR5-tropic isolates in the presence of DTG. These Env mutants exhibit reduced susceptibility to DTG, with effects on replication kinetics and Env structure that are HIV-1 strain-dependent. Finally, to examine a possible *in vivo* relevance of Env-mediated drug resistance, we performed single-genome sequencing of plasma-derived virus from five patients failing an integrase inhibitor-containing regimen. This analysis revealed the presence of several mutations in the highly conserved gp120-gp41 interface despite low frequency of resistance mutations in integrase. These results suggest a “stepping-stone” model whereby mutations in Env that enhance the ability of HIV-1 to spread via a cell-cell route increase the opportunity for the virus to acquire high-level drug resistance mutations in ARV-target genes.

Author summary

Although combination antiretroviral (ARV) therapy has proven highly effective in controlling the progression of HIV disease, drug resistance can be a major obstacle to long-term treatment, particularly in resource-limited settings. In most cases, resistance arises from the accumulation of mutations in the ARV-target genes; however, in some cases, resistance develops without ARV target-gene mutations. We previously reported that mutations in the HIV-1 envelope glycoprotein (Env) confer resistance to an integrase inhibitor. Here we investigated the mechanism of Env-mediated drug resistance and the possible contribution of Env to virological failure *in vivo*. We demonstrate that Env mutations can confer broad resistance to multiple classes of ARVs and define the effect of the Env mutations on Env subunit interactions and sensitivity to neutralizing antibodies. We also selected for drug resistance mutations in Env in clinically relevant HIV-1 isolates. We observed that many Env mutations accumulated in individuals failing integrase inhibitor therapy despite a low frequency of resistance mutations in integrase. Our findings suggest that broad-based, Env-mediated drug resistance may impact current and possibly future therapeutic strategies. Our findings also provide clues towards understanding how ARV-treated patients can experience virological failure without acquiring drug resistance mutations in ARV-target genes.

Introduction

More than thirty antiretrovirals (ARVs) are currently approved to treat HIV-1 infection [1]. These ARVs are categorized into five different classes based on their targets: (1) nucleoside analog reverse transcriptase inhibitors (NRTIs), (2) non-nucleoside analog reverse transcriptase inhibitors (NNRTIs), (3) integrase (IN) strand transfer inhibitors (INSTIs), (4) protease (PR) inhibitors (PIs) and (5) entry inhibitors (Ent-Is). The use of combinations of these ARVs (combination antiretroviral therapy; cART) has proven remarkably effective in controlling HIV disease progression and prolonging survival. However, resistance to ARVs emerges in some patients because of poor adherence, use of a suboptimal drug regimen, and/or lack of viral load monitoring, particularly in resource-limited settings. Transmitted drug resistance is therefore becoming an increasingly serious problem in many parts of the world [2]. In most cases, HIV drug resistance is the consequence of mutations that emerge in the viral genes targeted by the drugs, and the molecular and structural basis for such resistance has been extensively studied [2]. However, particularly in the case of PIs and INSTIs, virological failure can occur in the absence of target-gene mutations [3-10], indicating that mutations outside the target gene can contribute to drug resistance. For example, *in vitro* selection studies have demonstrated that mutations in the 3' polypurine tract (3' PPT) or in the viral long terminal repeat (LTR) can confer resistance to INSTIs [11, 12], and mutations in Gag and the envelope glycoprotein (Env) have been implicated in PI resistance [13, 14].

HIV-1 Env is translated as a gp160 precursor, which is cleaved by a cellular furin-like protease to generate noncovalently linked gp120 and gp41 subunits that are incorporated into virus particles as a heterotrimeric spike [15]. The binding of gp120 to CD4 on the target cell surface triggers a conformational rearrangement in Env that exposes the coreceptor (CCR5 or CXCR4)-binding site. Interaction of gp120 with coreceptor promotes the refolding of gp41 heptad repeat 1 and 2 (HR1 and 2) to form an antiparallel six-helix bundle that mediates the fusion of viral and cellular membranes, allowing viral entry into the cytosol of the target cell [16].

HIV-1 Env is the only viral protein exposed on the surface of the infected cell or viral particle; it is therefore the target of neutralizing antibodies (NAbs) that can block viral entry and induce antibody-mediated effector functions, such as antibody-dependent cellular cytotoxicity (ADCC). NAbs recognize conserved regions of the Env trimer, including (1) the CD4-binding site (CD4bs), (2) V2 apex, (3) V3 glycan, (4) gp120-gp41 interface, and (5) gp41 membrane-proximal external region (MPER) [17]. Single-molecule fluorescence resonance energy transfer (smFRET) analysis has revealed that Env trimers fluctuate between closed (state 1), intermediate (state 2) and open (state 3) conformations [18, 19]. The binding properties of NAbs are influenced by the conformational state of Env. For example, while many anti-V2 apex and anti-CD4bs Abs preferentially recognize the closed Env conformation, antibodies that bind the gp41 MPER and a CD4-induced epitope (CD4i) preferentially recognize Env conformations that arise after the engagement of gp120 with CD4. Therefore, NAbs are useful as molecular probes to investigate the structure and conformational dynamics of Env [18, 19].

HIV-1 can spread either via a cell-free route or by cell-cell transmission at points of cell-cell contact known as virological synapses (VSs). The formation of a VS is initiated by the interaction of Env on the infected cell and CD4 on the target cell [20-22], although Gag can accumulate at the VS even in the absence of Env [23]. The VS is stabilized by cellular adhesion proteins, such as LFA-1 and ICAM-1, and lipid raft microdomains and the actin cytoskeleton are also implicated in VS formation [24-26]. At least *in vitro*, cell-cell transfer of HIV-1 is markedly more efficient than cell-free infection [27-29]. HIV-1 transmission at a VS provides a higher multiplicity of infection (MOI) than cell-free infection, resulting in multiple copies of proviral DNA in the target cells [30-33]. This high MOI allows HIV-1 to overcome multiple barriers to infection, such as those imposed by ARVs, NAbs, and inhibitory host factors [32-38]. Although it is challenging to directly compare the relative contribution of cell-free infection and cell-cell transfer to HIV-1 dissemination and pathogenesis *in vivo*, several studies have suggested the importance of cell-associated virus in HIV-1 propagation in animal models of HIV-1 infection. Intravital imaging using humanized mice has demonstrated that HIV-1-infected T-cells are motile in lymph nodes and spleen, and form transient, Env-dependent adhesive contacts that may facilitate cell-cell viral transfer [39,

40]. In addition, multicopy transmission of HIV-1 as foci within lymphoid tissue has been reported in humanized mice [30, 40]. Inhibition of egress of lymphocytes reduced systemic dissemination of HIV-1, suggesting that migration of infected cells plays an important role in virus spread to other organs [39]. Electron tomography and immunofluorescence analyses in gut lymphoid tissues and bone marrow of humanized mice have provided support for both cell-free and cell-cell modes of HIV-1 transmission [41-43]. If cell-cell transfer, and the resulting higher MOI, is a common occurrence *in vivo* one would expect to find large numbers of multiply infected cells in HIV-1-infected individuals. This has been observed in some [44-46] but not other [47] studies. Further analysis will be needed to understand the importance of cell-cell transfer in viral dissemination *in vivo*.

We previously reported that HIV-1 evades blocks to virus replication by acquiring Env mutations that enhance the capacity of the virus to spread via cell-cell transmission [48]. By propagating HIV-1 mutants containing substitutions in the p6 domain of Gag that severely delay virus replication [49], we selected for second-site compensatory mutations Env-Y61H and P81S in gp120 and the Env-A556T mutation in gp41. These Env mutations decrease the sensitivity of the virus to the highly potent INSTI dolutegravir (DTG). Moreover, propagation of HIV-1 in the presence of DTG led to the selection of the DTG-escape mutant Env-A539V in the absence of any mutations in IN. These four Env mutations cluster within the C1 domain of gp120 and the HR1 domain of gp41 (Fig 1), which have been shown through mutagenesis and structural studies to be critical for the stability of gp120-gp41 association in the unliganded (non-CD4-bound) state [50-52]. These results suggest that Env mutations that increase cell-cell spread may alter the stability of the gp120-gp41 interaction and demonstrate that mutations in Env can confer resistance to an ARV, at least in a subtype B, CXCR4-tropic, laboratory-adapted HIV-1 strain. Whether Env-mediated drug resistance occurs in clinical HIV-1 isolates is unclear because Env from laboratory-adapted and primary HIV-1 strains differs in significant functional and structural aspects. Laboratory-adapted isolates often sample the open Env conformation and are more sensitive to NAbs compared to primary isolates, as *in vitro* adaptation of HIV-1 in the absence of immune selective pressure often leads to the emergence of neutralization-sensitive variants [18, 53, 54]. In addition, laboratory-

142 adapted isolates are more sensitive to soluble CD4 (sCD4) than primary isolates. sCD4 inhibits HIV-1
143 entry not only by competing with CD4 on the target cell, but also by inducing the shedding of gp120 from
144 the surface of viral particles and infected cells. Env complexes from laboratory-adapted isolates are more
145 prone to sCD4-induced gp120 shedding compared to primary isolates [55-57], indicating that Env
146 stability differs between laboratory-adapted and primary isolates.
147 In the present study, we examined whether our previously described Env mutations confer
148 resistance not only to DTG but also to other classes of ARVs. To evaluate the impact of the Env
149 mutations on the conformation and stability of the Env complex, we examined their effects on sensitivity
150 to NAbs and on gp120 shedding. To further characterize the mechanism of Env-mediated drug resistance,
151 we obtained Env mutants through *in vitro* selection experiments by propagating clinically relevant HIV-1
152 clones in the presence of DTG and analyzed the phenotypes of the selected Env mutants. Finally, to
153 address the possible *in vivo* relevance of Env-mediated drug resistance, we used single-genome
154 sequencing to compare viral sequences obtained from the plasma of individuals failing a raltegravir
155 (RAL)-containing regimen. The results indicate that Env mutations confer resistance across a broad
156 range of ARVs *in vitro*, and that the NL4-3 Env mutations decrease gp120 shedding and alter the
157 sensitivity of Env to NAbs. Finally, we show that in some individuals failing a RAL-containing regimen
158 in the absence of resistance mutations in IN, changes arise at the highly conserved gp120-gp41 interface,
159 as observed during INSTI escape *in vitro*.
160

Results

The A539V mutation in gp41 provides a replication advantage over WT NL4-3 in the presence of multiple classes of ARVs.

We previously reported that the Env-A539V mutation provides resistance to the INSTI DTG [48]. To examine whether Env-A539V also provides a selective replication advantage in the presence of other ARVs, the SupT1 T-cell line was transfected with the WT NL4-3 molecular clone or the Env-A539V derivative in the absence or presence of various concentrations (0.1 – 3,000 nM) of a panel of ARVs. Replication kinetics were monitored by measuring the RT activity in the cell culture media. Consistent with our previous report [48], Env-A539V exhibited faster replication kinetics compared to WT in the absence of drugs (Fig 2). Whereas replication of WT NL4-3 was largely inhibited in the presence of 3.0 nM DTG, Env-A539V could replicate, albeit with delayed kinetics (Fig 2A). By calculating the DTG IC_{50} based on the RT activity at the peak of replication in the absence of drugs, we found that Env-A539V showed 8.1-fold resistance to DTG relative to WT (Fig 2I). We also examined the sensitivity of Env-A539V to another INSTI, raltegravir (RAL). Env-A539V could replicate in the presence of 10 nM RAL and showed 5.4-fold resistance relative to WT NL4-3 (Figs 2B and I). We also measured replication kinetics of Env-A539V in the presence of the NNRTI efavirenz (EFV) and the NRTI emtricitabine (FTC). Whereas replication of WT NL4-3 was strongly inhibited in the presence of 3.0 nM EFV or 30 nM FTC, Env-A539V could still replicate at these concentrations (Figs 2C and D). IC_{50} calculations showed that Env-A539V exhibited 28- and 5.4-fold resistance against EFV and FTC, respectively (Fig 2I). Next, we examined the impact of PIs on the replication kinetics of Env-A539V. While replication of WT NL4-3 was strongly inhibited in the presence of 3.0 nM nelfinavir (NFV), the Env-A539V mutant could replicate and exhibited 24-fold resistance (Figs 2E and I). We also examined the sensitivity of Env-A539V to the allosteric integrase inhibitor (ALLINI), BI-224436, which induces aberrant IN multimerization and impairs the interaction between IN and the cellular cofactor LEDGF/p75 [58]. As shown in Fig 2F, Env-A539V caused a small but statistically significant reduction in the sensitivity to BI-224436 relative to WT

NL4-3 (2.3-fold resistance, Fig 2I). These data demonstrate that Env mutations can overcome inhibition imposed by multiple classes of ARVs targeting not only post-entry steps, but also the maturation step of the HIV-1 replication cycle.

It has been suggested that entry inhibitors (Ent-Is) are effective in the context of cell-cell transmission [59, 60]. In addition, several studies have shown that Env mutations selected in the presence of Ent-Is altered viral sensitivity to other anti-Env agents [61-64]. These findings raise the possibility that Env mutations selected in the presence of ARVs might alter the viral sensitivity to Env-targeted inhibitors. To examine this question, we measured replication kinetics in the presence of the fusion inhibitor T-20 and the attachment inhibitor BMS-378806. Interestingly, these Ent-Is could efficiently suppress replication of both WT NL4-3 and Env-A539V with no statistically significant differences in antiviral IC_{50} in a multi-cycle spreading infection (Figs 2G – I). These observations suggest that Ent-Is could suppress the replication of Env mutants selected under the pressure of ARVs targeting the viral enzymes.

The Env-A539V mutation does not alter drug sensitivity in cell-free infection.

We previously proposed that Env mutations that confer resistance to ARVs do so by enhancing the efficiency of cell-cell transfer [48]. Based on this hypothesis, the Env mutations would not be predicted to confer resistance in the context of cell-free infectivity. To test this hypothesis, we measured the infectivity of WT NL4-3 and the Env-A539V mutant in the TZM-bl indicator cell line. For early-acting inhibitors (INSTI, NNRTI, NRTI and Ent-Is), infection of TZM-bl cells was performed in the presence of the drugs. For late-acting inhibitors (PI and ALLINIs), virus stocks were produced in the presence of the inhibitors, and then used to infect the TZM-bl cells. As we reported previously [48], Env-A539V showed comparable cell-free infectivity relative to WT NL4-3 in the absence of inhibitor (Fig 3A and Table 1). Consistent with the hypothesis that the reduced ARV sensitivity of the Env-A539V mutant is conferred at the level of cell-cell transmission, WT and Env-A539V infectivity was reduced to the same extent by the inhibitors (Figs 3B – I, and Table 1). Interestingly, Env-A539V did not alter susceptibility to

211 either T-20 or BMS-378806, suggesting that Ent-Is efficiently suppress both cell-free infection and cell-
212 cell transmission of HIV-1.

213

214 **Table 1. IC_{50} values in cell-free infection for WT NL4-3 and the A539V variant**

ARV classes/NAb epitopes	Drug/NAbs	IC_{50} (nM[a], μg/ml[b], dilution factors[c], mean ± SE)			
		WT	Env-A539V	Fold changes	Significance
INSTIs	DTG[a]	3.3 ± 0.65	3.0 ± 0.72	0.91	ns
	RAL[a]	11 ± 0.94	15 ± 1.6	1.4	ns
NRTIs	FTC[a]	558 ± 10	511 ± 30	0.92	ns
NNRTIs	EFV[a]	1.2 ± 0.31	1.4 ± 0.27	1.2	ns
PIs	NFV[a]	46 ± 21	28 ± 3.1	0.61	ns
ALLINIs	BI-224436[a]	14 ± 2.0	14 ± 1.9	1.0	ns
Ent-Is	BMS-378806[a]	2.3 ± 0.66	2.9 ± 0.54	1.3	ns
	T-20[a]	42 ± 13	38 ± 2.9	0.90	ns
	AMD3100[a]	0.91 ± 0.070	0.77 ± 0.032	0.85	ns
	sCD4[b] (0 hr)	0.40 ± 0.031	0.97 ± 0.14	2.4	*
	sCD4[b] (2 hr)	0.30 ± 0.085	1.1 ± 0.21	3.7	**
anti-CD4 Ab	SIM.4[c]	88 ± 30	79 ± 24	0.90	ns
anti-V2 apex Ab	PG16[b]	13 ± 12	0.62 ± 0.30	0.048	ns
	PGT145[b]	1.3 ± 0.087	0.39 ± 0.22	0.30	*
anti-V3 glycan Ab	2G12[b]	1.3 ± 0.33	1.3 ± 0.54	1.0	ns
	PGT121[b]	> 10	> 10	N.D.	N.D.
anti-CD4bs Ab	VRC01[b]	0.11 ± 0.0070	0.11 ± 0.013	1.0	ns
	F105[b]	1.4 ± 0.51	4.3 ± 0.43	3.1	**
anti-CD4i Ab	17b[b]	0.81 ± 0.28	22 ± 12	27	*
anti-V3 loop Ab	447-52D[b]	0.39 ± 0.096	11 ± 2.6	28	***
anti-gp41 MPER Ab	10E8[b]	0.067 ± 0.020	0.12 ± 0.063	1.8	*
anti-gp120-gp41 interface Ab	35O22[b]	0.062 ± 0.024	0.13 ± 0.026	2.1	ns

215 TZM-bl cells were exposed to 100 $TCID_{50}$ of the indicated virus in the presence of ARVs or NAbs. Data
216 are shown as mean ± SE. Statistical analysis was performed using an unpaired *t*-test. ns, not significant; *p*-
217 values < 0.001 (***), < 0.01 (**), < 0.05 (*). N.D.; not determined.

218 [a] nM

219 [b] μg/ml

220 [c] dilution factors

221

222 **The Env-A539V mutation increases viral resistance to EFV when coupled with the RT-**
223 **Y188L mutation.**

224 To examine whether mutations in Env can increase the level of resistance conferred by drug
225 target gene mutations, we tested EFV resistance of the RT-Y188L mutant [65] in the context of either WT
226 or A539V Env. As shown in Fig 4A (left panel), RT-Y188L showed a modest delay in replication
227 compared to WT in the absence of EFV, indicating that this RT mutation confers a small fitness defect.
228 This replication defect was rescued by Env-A539V, consistent with our earlier finding that Env mutations
229 can rescue the replication defect conferred by a mutation in IN [48]. In the presence of 1.0 mM EFV, the
230 Env-A539V mutation was able to markedly enhance the replication kinetics of the RT-Y188L mutant (Fig
231 4A, right panel), a result that was confirmed over a broad range of EFV concentrations (Figs 4B and D).
232 In contrast to the results in the multi-cycle spreading infection (Fig 4B), the Env-A539V mutation did not
233 increase EFV resistance of RT-Y188L in a single-cycle infectivity assay (Figs 4C and D). Taken
234 together, these results demonstrate that, in the context of a spreading infection in which virus transmission
235 can take place via cell-cell transfer, an Env mutation can significantly increase the resistance conferred by
236 a mutation in an ARV-target gene.

237

238 **NL4-3 Env mutations that overcome blocks to HIV-1 replication in spreading infections**
239 **stabilize the gp120-gp41 interaction.**

As shown in Fig 1B, our previously reported Env mutations, which we selected for their ability to overcome blocks to virus replication in multi-cycle spreading infections, are located in the C1 domain of gp120 and the HR1 region of gp41. These domains of Env have been shown in mutagenesis and structural studies to be critical for the stability of the gp120-gp41 association in the unliganded state [50-52, 62, 66]. To provide clues regarding the mechanism by which Env mutations enhance the capacity of HIV-1 to spread via cell-cell transfer, we examined their impact on gp120-gp41 association. It is known that sCD4 induces gp120 shedding from virus particles [57]; we therefore incubated purified virions with sCD4 at 37°C for 2 hrs, and then measured the amount of particle-associated gp120 and p24 by western blotting. The amount of gp160 in virions was used as a control, as it is not shed from virions and can be detected with the same antibody used to detect gp120. As expected, levels of gp120 associated with WT NL4-3 particles were decreased in a dose-dependent fashion by sCD4 treatment (0.3 – 10 μg/ml). By contrast, the mutations in both gp120 (Env-Y61H and P81S) and gp41 (Env-A539V and A556T) showed significantly reduced sCD4-induced gp120 shedding (Fig 5A). To quantify this effect, we calculated the 50% effective concentration (EC_{50}) of sCD4-induced shedding. While the EC_{50} of sCD4-induced gp120 for WT NL4-3 was 0.99 μg/ml sCD4, the EC_{50} for the Env-P81S and the other Env mutants was 3.5 and > 10 μg/ml, respectively (Fig 5B). To examine the interaction between sCD4 and a representative Env mutant, we measured the sensitivity of Env-A539V infectivity to sCD4 (Fig 5C). Env-A539V showed a 3.7-fold resistance to sCD4 relative to WT. Moreover, the IC_{50} of sCD4 against Env-A539V was 1.1 μg/ml (Table 1), which is more than about 10-fold less than the EC_{50} of sCD4-induced gp120 shedding, suggesting that sCD4 could bind to mutant Env at lower concentrations than needed for gp120 shedding, leading to inhibition of viral entry. To further characterize the intrinsic stability of mutant Envs, we also performed a time-dependent gp120 shedding assay by incubating viruses at 37°C for up to 5 days (Fig 5D). The levels of gp120 on WT NL4-3 particles were decreased during the 5-day incubation period. The Env mutations significantly reduced time-dependent gp120 shedding (Fig 5E). Whereas the half-life of WT NL4-3 gp120 shedding was 2.6 days, that of the Env mutants was > 5 days. These data suggest that the NL4-3 Env mutations stabilize the gp120-gp41 interaction.

The Env-A539V mutation reduces sensitivity to neutralizing antibodies (NAbs) that recognize the CD4-induced Env conformation.

smFRET analysis revealed that the HIV-1 Env trimer samples three conformational states [18, 19]. It has been suggested that anti-Env NAbs and Env-targeting entry inhibitors display preferences for specific Env conformations [18, 19, 67] and that the gp41 ectodomain can modulate the conformational dynamics of Env [52, 62, 66]. To probe the impact of the Env-A539V mutation on Env conformation, we examined the sensitivity of Env-A539V to a panel of NAbs (Fig 6). We used three groups of NAbs: The first group (Figs 6A – E), which included VRC01 (specific for the CD4bs), PGT145, PG16 (specific for the V2 apex), 2G12 and PGT121 (V3-glycan-specific), preferentially bind to the unliganded, closed Env conformation [68-71]. The second group (Fig 6F) included 35O22, which is specific for the gp120-gp41 interface and shows no conformational preference [72]. The third group (Figs 6G - J) included F105 (CD4 bs-specific), 17b (specific for the CD4i epitope), 447-52D (V3 loop), and 10E8 (gp41 MPER), preferentially target the CD4-bound Env conformation [73-76]. Although the Env-A539V mutation is not located within the epitopes of the NAbs used in this analysis, it altered the sensitivity to several NAbs, with reduced sensitivity to F105 (3.1-fold), 447-52D (28-fold), 17b (27-fold), and 10E8 (1.8-fold) and increased (33-fold) sensitivity to PGT145 (Table 1). To further probe the effect of the Env-A539V mutation on Env conformation, we compared NAb binding to Env on 293T cells by flow-cytometry. As indicated in Figs 6M and N, 17b and 10E8 less efficiently bind to Env-A539V relative to WT Env. In contrast, PGT145 and PG16 bind the mutant Env to a similar extent as WT NL4-3 Env (Figs 6O and P). These data suggest that the Env-A539V mutation stabilizes the closed Env conformation. We also examined sensitivity to SIM.4 (an anti-CD4 Ab) [77] and AMD3100 (a CXCR4 antagonist) [78] to evaluate the impact of the Env-A539V mutation on Env function in HIV-1 entry. As shown in Figs 6K and L, Env-A539V showed comparable sensitivity to SIM.4 and AMD3100 compared to WT NL4-3, suggesting that this mutation does not alter CD4 and CXCR4 dependency.

Env mutations confer ARV resistance in the context of CCR5-tropic HIV-1.

To examine whether Env-mediated resistance to ARVs occurs in strains of HIV-1 other than the CXCR4-tropic, lab-adapted strain NL4-3, we propagated the CCR5-tropic clone NL(AD8) [79] in the SupT1huR5 T-cell line, which expresses high levels of human CCR5, in the presence of DTG. Treatment of transfected SupT1huR5 cultures with 6.0 nM DTG markedly delayed NL(AD8) replication, but at 31 days post-transfection we observed a peak of replication (Fig 7A). Sequencing of the putative escape mutant indicated the absence of any mutations in IN but revealed the presence of an Env-N654K mutation in gp41 HR2 (Fig 7B). Asn at position in 654 is highly conserved (99.76%) in subtype B. To examine whether the Env-N654K mutation in NL(AD8) confers resistance to DTG, we introduced the mutation in WT NL(AD8) and examined replication kinetics in the presence of DTG (Fig 7C). Interestingly, this mutant exhibits faster replication kinetics than WT and can still replicate in the presence of 300 nM DTG (Fig 7C, left panel). IC_{50} calculations indicate that the Env-N654K mutation confers 30-fold resistance to DTG relative to WT NL(AD8) (Fig 7D). As observed with several of the Env mutations selected in our previous study [48], the Env-N654K mutation impairs single-cycle infectivity (Fig 7E) and does not confer DTG resistance in the context of cell-free infection (Fig 7F and Table 2). These results are all consistent with the hypothesis that, as with the mutations selected in the context of NL4-3, the NL(AD8) Env-N654K mutation confers DTG resistance by enhancing the efficiency of cell-cell transfer.

Table 2. IC_{50} values in cell-free infection for NL(AD8) variants

ARV classes/NAb epitopes	Drug/NAbs	IC_{50} (nM[a], µg/ml[b], dilution factors[c], mean ± SE)			
		WT	Env-N654K	Fold changes	Significance
INSTIs	DTG[a]	4.9 ± 0.71	6.2 ± 2.7	1.3	ns
Ent-Is	BMS-378806[a]	3.0 ± 0.24	2.8 ± 0.59	0.93	ns
	T-20[a]	2,938 ± 724	797 ± 225	0.27	**
	MVC[a]	2.3 ± 0.36	1.1 ± 0.33	0.48	*
	sCD4[b] (0 hr)	4.1 ± 0.23	1.3 ± 0.42	0.32	***
	sCD4[b] (2 hr)	3.6 ± 0.25	1.4 ± 0.31	0.39	***
anti-CD4 Ab	SIM.4[c]	113 ± 6.5	371 ± 44	3.3	***

anti-V2 apex Ab	PG16[b]	0.040 ± 0.020	0.11 ± 0.053	2.8	ns
	PGT145[b]	0.068 ± 0.0060	0.062 ± 0.014	0.91	ns
anti-V3 glycan Ab	2G12[b]	> 30	> 30	N.D.	N.D.
	PGT121[b]	0.043 ± 0.0026	0.036 ± 0.0073	0.84	ns
anti-CD4bs Ab	VRC01[b]	0.40 ± 0.076	0.46 ± 0.14	1.2	ns
	F105[b]	> 10	> 10	N.D.	N.D.
anti-CD4i Ab	17b[b]	> 30	> 30	N.D.	N.D.
anti-gp41 MPER Ab	10E8[b]	0.47 ± 0.075	0.050 ± 0.012	0.11	***
anti-gp120-gp41 interface Ab	35O22[b]	4.1 ± 2.2	0.074 ± 0.037	0.018	ns

TZM-bl cells were exposed to 100 $TCID_{50}$ of the indicated virus in the presence of ARVs or NAbs. Data are shown as mean ± SE. Statistical analysis was performed using an unpaired *t*-test. ns, not significant; *p*-values < 0.001 (***), < 0.01 (**), < 0.05 (*). N.D.; not determined.

[a] nM

[b] μg/ml

[c] dilution factor

We also propagated the subtype C, CCR5-tropic transmitted-founder isolate K3016 [80] in the presence of DTG. We identified the Env-T529I mutation in gp41 HR1, which is located at the same position as NL4-3 Env-A539V (S1A and B Figs). This mutant showed 2.8-fold-reduced sensitivity to DTG, although its replication was delayed relative to that of WT K3016 (S1C and D Figs). These results indicate that Env-mediated drug resistance *in vitro* can occur in clinically relevant HIV-1 strains independent of co-receptor usage and subtype.

To examine whether the Env-A539V mutation, which was originally selected in the context of NL4-3 [48], would also confer ARV resistance in the context of another viral isolate we introduced this mutation into the NL(AD8) molecular clone. In contrast to the phenotype of this mutant in NL4-3, the NL(AD8) Env-A539V mutant exhibited delayed replication in the absence of DTG and caused an increase (3.1-fold) in DTG sensitivity in multi-cycle spreading infections. Moreover, the cell-free

326 infectivity of the NL(AD8) Env-A539V mutant was reduced relative to that of WT NL(AD8) (Figs 7C -
327 E). These data demonstrate that the impact of Env mutations on replication kinetics and drug sensitivity
328 can be HIV-1 strain-dependent.

329 Next, to examine the impact of the Env-N654K mutation on the conformation and neutralization
330 properties of NL(AD8) Env, we examined the sensitivity of this mutant to a panel of NAbs (Fig 8 and
331 Table 2). Compared to NL4-3, NL(AD8) is more susceptible to NAbs, such as PGT121, PG16 and
332 PGT145, that preferentially recognize the closed Env conformation (S2 Fig, and Tables 1 and 2).
333 Conversely, NL(AD8) is resistant to 17b (S2 Fig, and Tables 1 and 2) and F105 (Table 1). These results
334 suggest that NL(AD8) tends to sample the closed Env conformation relative to NL4-3. NL(AD8) Env-
335 N654K increased sensitivity to 35O22 (56-fold) and 10E8 (9.1-fold) (Figs 8E and G, and Table 2).
336 Because the effects of N654K on the sensitivity to other NAbs are minimal, this mutation may affect the
337 local structure of HR2 and the MPER rather than the global structural dynamics of NL(AD8) Env. We
338 also examined sensitivity to several entry inhibitors (Figs 8H – L and Table 2). Env-N654K slightly
339 increased sensitivity to SIM.4, maraviroc (MVC; a CCR5 antagonist) and T-20. Moreover, Env-N654K
340 increased the sensitivity to sCD4. Unlike NL4-3 (S2J Fig), incubation time did not affect the
341 susceptibility of Env-N654K to sCD4 (Fig 8H and S2J Fig). This observation suggests that sCD4-
342 induced gp120 shedding is minimal in the NL(AD8) strain, consistent with previous reports for non-lab-
343 adapted isolates [55-57]. Indeed, we did not observe sCD4-induced gp120 shedding from either WT or
344 Env-mutant particles at sCD4 concentrations up to 10 μg/ml (S3A, C and E Figs.). We also examined
345 time-dependent gp120 shedding (S3B and D Figs). In contrast to NL4-3 (Figs 5D and E, and S3F Fig),
346 only minimal gp120 shedding was observed for NL(AD8) Env over a 5-day incubation period at 37°C,
347 and there was no significant difference in shedding between WT and Env-N654K NL(AD8) Env (S3B
348 and D Figs).

349

Sequence analysis of IN- and Env-coding regions of viruses from individuals failing a RAL-containing regimen.

Our results indicate that Env-mediated drug resistance can occur in clinically relevant HIV-1 strains *in vitro*. However, whether Env mutations contribute to drug resistance *in vivo* is unclear. To address this question, we used single-genome sequencing to compare viral sequences obtained from the plasma of participants failing a RAL-containing regimen in the SELECT study [5]. The aim of the SELECT study was to examine whether RAL with boosted lopinavir (LPV) would be non-inferior to boosted LPV with NRTIs. By 48 weeks of treatment, 10.3% of 258 participants treated with the RAL-containing regimen experienced virological failure, defined here as the inability to achieve a viral load under 400 copies/ml at two consecutivetime points at or after 24 weeks of treatment. By the end of the follow-up in this study, ten participants developed new resistance mutations in IN, including IN-N155H. In the present study, we compared changes in the sequences of IN- and Env-coding regions from five participants who experienced viral rebound (Table 3). These participants were infected with subtype C, CCR5-tropic strains. Each participant had therapeutic plasma concentrations of RAL (> 33 ng/ml) at the time of virological failure. No resistance mutations in IN were detected at day 0, (Table 3). While we identified the IN-N155H mutation in participant identifier (PID) A5 with high frequency (73%), PID A1, A3 and A5 had resistance mutations in IN with low frequency (Table 3), suggesting that virological failure may have occurred in these participants as a result of mutations elsewhere in the HIV-1 genome.

Table 3. Information on study participants failing a RAL-containing regimen.

Participant identifier (PID)	Sampling timepoint		HIV-1 RNA (copies/ml)	RAL conc. (ng/ml)	IN accessory/resistance mutations
A1	Pre-ART	Day 0	805,710	-	No mutations detected

	Early RAL failure	Day 181	570	990	Not determined
	Late RAL failure	Day 250	11,335	89	T97A (33%), **N155H (5.6%)**
A2	Pre-ART	Day 0	17,450	-	No mutations detected
	Late RAL failure	Day 195	1,772	93	No mutations detected
A3	Pre-ART	Day 0	1,329,415	-	No mutations detected
	Early RAL failure	Day 178	433	965	Not determined
	Late RAL failure	Day 196	1,139	3,371	**F121Y (14%)**
A4	Pre-ART	Day 0	1,617,523	-	No mutations detected
	Early RAL failure	Day 175	7,208	1,142	**E138K (2.7%), N155H (73%)**
	Late RAL failure	Day 199	9,918	480	Not determined
A5	Pre-ART	Day 0	30,206	-	No mutations detected
	Late RAL failure	Day 194	18,806	2,729	**G163K (4.8%)**

Samples are derived from the SELECT study [5].

RAL resistance mutations are indicated in bold.

Evaluation of the Env-coding region before treatment and during virologic failure indicated the presence of many changes in gp120 and gp41 that emerged or were selected with failure. Most of changes

375 in gp120 were located in highly variable regions, such as the variable loops (V1/V2, V4 and V5 loop),
376 and the C3 region (data not shown). Because these regions contain immunodominant epitopes of subtype
377 C Env, mutations in these regions may have been driven by immune pressure [81, 82]. Although we did
378 not identify mutations at the same positions observed in our *in vitro* studies, we observed an accumulation
379 of mutations in the gp120 C1 domain and gp41 ectodomain in PID A1, A3, A4 and A5 (Figs 9A and B).
380 The frequency of most of the mutations increased significantly with viral rebound. Although we identified
381 a number of Env mutations in PID A2, the frequency of mutations before RAL therapy was similar to that
382 after viral rebound although the RAL-containing regimen decreased viral load before viral rebound (data
383 not shown and Table 3). In many cases, amino acid residues were replaced with more conserved residues;
384 however, we did identify changes to residues with very low prevalence, such as R577K (gp41 HR1) and
385 L602R (gp41 HR2). Some mutated positions in the gp41 ectodomain were identified in several
386 participants (Figs 9A and B). The observation of changes arising in highly conserved positions at the
387 gp120-gp41 interface – a region in which, based on our data, mutations that confer ARV resistance *in*
388 *vitro* cluster – in the absence of drug-resistance mutations in IN, suggests the possibility that these gp41
389 changes may have contributed to virological failure in a subset of participants in the study. Further
390 analysis will be needed to explore this hypothesis in more detail.
391
392

Discussion

In this study, we demonstrate that the NL4-3 Env-A539V mutant, which was selected in the presence of DTG, confers broad resistance to multiple classes of ARVs in multi-cycle spreading infections. This Env mutation also increases resistance to ARVs when coupled with ARV target-gene mutations, again in the context of spreading infections. However, the Env mutation does not alter ARV susceptibility in cell-free infection. The results demonstrate that Env mutations clustered at the gp120-gp41 interface can confer broad resistance by enhancing the ability of HIV-1 to spread via a cell-cell route of transmission. Interestingly, NL4-3 Env mutants exhibiting an enhanced ability to spread via cell-cell transmission have more stable and closed Env conformations compared to WT NL4-3. By propagating CCR5-tropic HIV-1 strains NL(AD8) and K3016 in the presence of DTG, we obtained gp41 ectodomain mutations Env-N654K and Env-T529I, respectively. We demonstrate that these Env mutations reduce susceptibility to DTG in multi-cycle spreading infection as observed for the NL4-3 Env mutants, indicating that Env-mediated drug resistance can occur in non-laboratory-adapted HIV-1 strains. However, the effects of the Env mutations on replication kinetics and Env structure are HIV-1 strain-dependent. Finally, we performed single-genome sequencing analysis of the IN- and Env-coding regions of viruses from infected individuals failing a RAL-containing regimen. We observed that many mutations accumulated in the Env- but not IN-coding region in most study participants. While most of the gp120 changes that arose *in vivo* were located in highly variable regions, a number of changes in the gp41 ectodomain were observed at the highly conserved gp120-gp41 interface, as observed *in vitro*.

Several studies have demonstrated that cell-cell transfer is associated with a reduced susceptibility to ARVs relative to cell-free infection [32-34]. We previously proposed a model, consistent with other findings [33], whereby Env mutations that enhance cell-cell transmission increase the MOI following viral transfer across the VS; concentrations of DTG that are sufficient to inhibit cell-free infection by these mutants are therefore insufficient to block their cell-cell transmission [48]. Based on this model, the selected Env mutations would be predicted to confer resistance to multiple ARVs

418 independent of their mode of action, and should confer resistance in the context of a spreading, but not
419 cell-free, infection. Indeed, the NL4-3 Env-A539V mutant selected in the presence of DTG exhibits
420 broad resistance to a number ARVs including INSTIs, NRTIs, NNRTIs and PIs in spreading replication
421 assays but not in cell-free infectivity assays. These observations suggest that the broad resistance
422 conferred by the HIV-1 Env mutations will affect susceptibility to not only the currently approved ARVs,
423 but also potentially to next-generation drugs.

424 In contrast to the other classes of ARVs, Env-A539V is sensitive to two types of Ent-Is: a fusion
425 inhibitor (T-20) and an attachment inhibitor (BMS-378806). Previous studies have shown that Ent-Is
426 targeting CD4 or co-receptor are effective in blocking cell-cell transmission [34, 60, 83]. While some
427 CD4bs-targeting agents inefficiently inhibit cell-cell transmission, anti-gp41 MPER Abs and T-20 are
428 effective [60, 84]. These observations suggest that accessibility of epitopes or time of action may be
429 important factors for the efficacy of Ent-Is in blocking cell-cell transfer. Interestingly, the Env-A539V
430 mutation has been reported to emerge in the presence of low concentrations of fusion inhibitors *in vitro*;
431 however, this mutation does not confer resistance to the fusion inhibitor and reverted back to WT at high
432 inhibitor concentration [85]. Overall, our findings imply that including Env-targeted inhibitors in a cART
433 regimen may help prevent the emergence of the type of broadly resistance-conferring Env mutations
434 described here and previously [48].

435 Virological failure has been observed in patients on PI-containing regimens in the absence of PI-
436 resistance mutations in PR or in the vicinity of Gag cleavage sites [7, 86-89]. Likewise, recent studies
437 have demonstrated that viral rebound can occur in individuals on INSTI-containing therapies without the
438 emergence of INSTI-resistance mutations in IN [5, 6]. In some studies [90, 91] there are concerns about
439 whether the infected individuals remained compliant (i.e., whether suppressive concentrations of the
440 inhibitors were maintained), but in other studies (e.g., La Rosa et al., 2016 [5]) the maintenance of
441 adequate plasma drug concentrations was experimentally verified. In some cases in which target-gene
442 mutations were identified in the treated individuals experiencing virological failure, the resistance
443 mutations identified conferred only low-level resistance [3-10]. These findings suggest that mutations

outside the *pol*-coding region (and not around Gag cleavage sites, in the case of PIs) also contribute to virological failure in association with the target-gene mutations. Mutations in the cytoplasmic tail of gp41 have been previously proposed to contribute to PI resistance *in vivo* [13], potentially reflecting the role of virion maturation in Env-mediated viral entry [92, 93], and mutations in the gp41 HR region have also been observed in association with PI failure although the contribution of the mutants to virological failure is still unclear [9]. In addition to mutations in IN, it has also been reported that mutations in the 3' PPT contribute to INSTI failure both *in vitro* and *in vivo* [12, 94]. We demonstrate here that the Env-A539V mutation rescues the defect in virus replication imposed by the RT-Y188L mutation [65] and increases the resistance of this RT mutant to EFV in multi-cycle spreading but not cell-free infection. These observations indicate that Env mutations can increase resistance conferred by mutations in the ARV-target gene by enhancing viral cell-cell transmission. Mathematical modeling suggests that cell-cell transmission increases the probability that NAb-resistance mutations will emerge, relative to cell-free infection, as a result of reduced NAb potency in the context of cell-cell transmission [84]. As shown in Fig. 2, Env-A539V provides a replication advantage over WT NL4-3 in the presence of ARVs, suggesting that mutations in Env such as those described here may facilitate the acquisition by the virus of resistance mutations in ARV-target genes. According to this "stepping stone" model, by facilitating virus replication in the presence of ARVs the Env mutations would facilitate the emergence of high-level resistance mutations in ARV-target genes. Additional studies will be needed to investigate the role of HIV-1 Env in the development of high-level drug resistance.

We observed that Env mutations in the NL4-3 strain reduce sCD4-induced and time-dependent shedding of gp120 from viral particles. In addition, the Env-A539V mutation decreases sensitivity to NAbs preferring the CD4-bound conformation, whereas this mutant is more susceptible to PGT145, which recognizes the closed Env conformation. These observations suggest that the NL4-3 mutant Envs are more closed and stable on viral particles compared to WT NL4-3 Env. Flow-cytometry analysis using Env-expressing cells indicates that the NAb-binding properties of the mutants largely parallel their neutralization properties, suggesting that mutant Envs on the surface of infected cells exhibit similar

conformational dynamics to those on viral particles. Because the NL4-3 Env-A539V mutation does not alter sensitivity to an anti-CD4 Ab or a CXCR4 antagonist, it is likely that the enhancement of cell-cell transfer is due to the increased probability of gp120-CD4 interactions, rather than the increased affinity of gp120 for CD4 or CXCR4. Our findings suggest that decreased gp120 shedding may contribute to enhanced Env-CD4 interactions at cell-cell contact sites. To better understand how Env mutations stabilize gp120-gp41 interactions, we generated structural models using the published Env structures (S4 and S5 Figs) [95, 96]. The models suggest that, relative to the WT, Env-A539V and A556T likely make additional gp120-gp41 contacts in the unliganded Env structure. In addition, the His at residue 61 in the Env-Y61H mutant is predicted to form a salt bridge with E558 in the gp41 HR1 domain (S4 Fig). These new contacts may contribute to stabilization of the gp120-gp41 interaction. In contrast, the Env-P81S mutation does not result in the formation of obvious new contacts in either the unliganded or CD4-bound conformation; however, this mutation disrupts the interaction between Env-P81 and Env-P79 in the CD4-bound conformation (S5 Fig). These two residues are located in a loop region of the α0 helix in the CD4-bound conformation. This helix is formed after CD4 binding and is suggested to have important roles in conformational rearrangements of Env [95]. Based on the results of our gp120 shedding assays, we hypothesize that the Env-P81S mutation may affect the folding of the CD4-bound gp120 structure, resulting in the mutant Env adopting a more closed conformation and reducing gp120 shedding. Our results provide new insights into the relationship between cell-cell transfer and the stability of the gp120-gp41 interaction.

We performed resistance analyses using the more clinically relevant HIV-1 strains NL(AD8) and K3016. We introduced the Env-A539V mutation into NL(AD8) and observed a different phenotype from that observed with this mutation in NL4-3. Whereas NL4-3 Env-A539V exhibited a faster-than-WT replication kinetics, NL(AD8) Env-A539V exhibited impaired replication kinetics and was more susceptible to DTG than WT NL(AD8). These results imply that the Env-A539V mutation will not emerge in the context of the NL(AD8) strain. However, DTG selection experiments led to the emergence of an Env-T529I mutation, which is located at the same position as NL4-3 Env-A539V, in the context of

the subtype C, CCR5-tropic transmitted-founder isolate K3016. Although this mutant replicated more slowly than WT K3016 it exhibited reduced susceptibility to DTG. These results highlight the context dependence of resistance-conferring Env mutations, consistent with the suggestion that residues in the gp41 ectodomain are functionally linked with gp120 and modulate conformational dynamics of Env in a strain-dependent manner [52, 62, 97, 98]. As shown in S2 and S3 Figs, the stability of the gp120-gp41 interaction and the conformational dynamics of NL(AD8) Env are different from those of NL4-3 Env, suggesting that the differences in intra- and interprotomer interactions of Env are likely to affect the viral phenotypes of the Env mutants in terms of their fitness and ability to confer broad ARV resistance.

Propagation of NL(AD8) in the presence of DTG led to the selection of the Env-N654K mutation in gp41 HR2. Like several of the selected NL4-3 Env mutations (this report and Van Duyne et al., 2019 [48]), the NL(AD8) Env-N654K mutation confers resistance to DTG and is highly fit in multi-cycle spreading infections, but is also profoundly defective in cell-free infectivity. These observations suggest that this mutant spreads predominantly via a cell-cell route as observed for the NL4-3 Env mutants. However, the effects of the NL(AD8) Env-N654K mutation on Env stability and conformational dynamics appear to be different from those of the NL4-3 Env mutants. This mutation increases sensitivity to the anti-CD4 Ab, MVC, and to sCD4, T-20 and anti-MPER Ab, suggesting that this mutation may alter Env conformational changes after CD4 binding. An Asn at Env-654 is highly conserved (99.76% in subtype B), and previous studies have shown that substitutions at this position decrease the affinity of HR2 for HR1, resulting in decreased cell-free infectivity and fusogenicity [99-101]. Several lines of evidence suggest that syncytium formation is tightly regulated at the site of cell-cell contact by viral and cellular factors [92, 93, 102]. Although the roles of syncytium formation in HIV-1 replication are still debated, the formation of large syncytia may negatively impact HIV-1 replication [102, 103]. Several studies have reported that mutations in Env arose in infected SupT1 cells and improved replication in the absence of syncytium formation [104-107]. As we previously reported, Env-Y61H, P81S and A556T in the NL4-3 strain enhance cell-cell transmission while impairing cell-free infectivity and fusogenicity, indicating that for these mutants reduced fusogenicity is associated with enhanced cell-cell transmission

522 capacity [48]. Additional studies will be needed to elucidate the precise mechanism of action of the Env-
523 N654K mutation.

524 To explore the possibility that Env-mediated ARV resistance may occur *in vivo*, we performed
525 single-genome sequence analysis using samples from the SELECT study [5], in which virological failure
526 occurred despite the maintenance of therapeutic levels of RAL in the plasma. Because INSTIs are highly
527 potent ARVs, several groups have investigated whether INSTI monotherapy would effectively suppress
528 viral loads in animal models and human participants [6, 108, 109]. These trials demonstrated that INSTI
529 monotherapy is not sufficient to suppress viral replication and viral loads rebounded. However, in many
530 cases, virological failure occurred in either the absence of mutations in IN, or in association with low-
531 frequency resistance mutations in IN [110]. Consistent with these observations, our single-genome
532 sequence analysis revealed that four of the five participants we analyzed had only low-frequency
533 resistance mutations in the IN-coding region. These results suggest that virological failure occurred in
534 these four participants as a result of mutations outside the Pol-coding region. As expected, we observed
535 that many Env mutations accumulated in less-conserved regions of Env, such as gp120 C3 and variable
536 loops, which are predominant targets for the Ab response [81, 82]. More interestingly, we also found that
537 several mutations in the gp41 ectodomain accumulated at the highly conserved gp120-gp41 interface, as
538 observed in our *in vitro* selection experiments, despite the fact that none of these changes was identical to
539 those selected *in vitro*. As shown in our *in vitro* studies, it is unlikely that the identical mutations observed
540 *in vitro* would emerge *in vivo* because the effects of the Env mutations on viral fitness and drug resistance
541 is viral strain dependent. It is interesting to note that viruses from PID A4, which had the IN-N155H
542 mutation with high frequency, had many changes in the gp120 C1 domain and the gp41 ectodomain
543 compared to viruses isolated from the other participants. A limitation of the current study is the relatively
544 small number of INSTI-failure samples analyzed. Larger numbers of samples will be needed to identify
545 specific mutational patterns associated with virological failure. In addition, other regions outside IN, such
546 as the 3' PPT, may also be associated with virological failure [12, 94]. Nevertheless, our findings provide

547 tantalizing support for the possibility that HIV-1 Env simultaneously evolves to escape from both NAbs
548 and ARVs in association with ARV target-gene mutations *in vivo*.

549 In summary, the findings of this study demonstrate that mutations in Env can contribute to broad
550 HIV-1 drug resistance *in vitro*. These findings offer mechanistic insights into Env-mediated drug
551 resistance *in vitro* and provide new clues to understand how HIV-1 develops high-level resistance to
552 ARVs *in vivo*.

553

Materials and Methods

Cell lines.

HeLa, HEK293T, and TZM-bl cells [111] were maintained in Dulbecco's modified Eagle medium (DMEM) supplemented with 10% fetal bovine serum (FBS) at 37°C in 5% CO_2. The SupT1 and SupT1huR5 T-cell lines [112] were cultured in RPMI-1640 medium supplemented with 10% FBS at 37°C in 5% CO_2. The SupT1huR5 T-cell line was a kind gift from James Hoxie, Perelman School of Medicine, University of Pennsylvania, Philadelphia, PA.

Compounds and neutralizing antibodies.

DTG and BMS-378806 were purchased from MedChemExpress. RAL, FTC, EFV, NFV, T-20, AMD3100 [78], MVC, SIM.4 [77], sCD4, PGT145 [69], PG16 [70], 2G12 [68], PGT121 [69], VRC01 [71], 447-52D [74], 17b [76], 10E8 [75], F105 [73], 35O22 [72], 16H3 [113], and HIV-Ig were obtained from the NIH AIDS Reagent Program, Division of AIDS, NIAID, NIH. BI-224436 [58] was a kind gift from Alan Engelman, Dana Farber Cancer Institute, Boston, MA.

Cloning and plasmids.

The full-length HIV-1 molecular clones pNL4-3 [114] and pNL(AD8) [79], and the subtype C transmitted founder viral clone CH185 (here denoted K3016, a kind gift from Christina Ochsenbauer and John Kappes, University of Alabama) [80] were used in this study. pBR-NL43-IRES-eGFP-nef$^+$ (pBR43IeG), a proviral clone that coexpresses Nef and eGFP from a single bicistronic RNA, was obtained from Frank Kirchhoff through the NIH AIDS Reagent Program [115, 116]. pNL4-3 and pBR43IeG clones bearing Env mutations (Env-Y61H, P81S, A539V and A556T) were described previously [48]. The pBR43IeG/KFS clone, which does not express HIV-1 Env, was described previously [48, 117]. pNL4-3 RT-Y188L [65] was constructed by an overlap PCR method using *SpeI* and *AgeI* restriction sites. pNL(AD8) Env mutants Env-A539V and N654K were constructed by an overlap PCR method using

579 *BamH*I and *Eco*RI restriction sites. Constructed plasmids were verified by Sanger DNA sequencing
580 (Psomagen).
581
582 **Preparation of virus stocks.**
583 The HEK293T and HeLa cell lines were transfected with HIV-1 proviral DNA using Lipofectamine 2000
584 (Invitrogen). At 48 hrs post-transfection, virus-containing supernatants were filtered through a 0.45 μm
585 membrane (Merck Millipore). The amount of virus in the supernatants was quantified by RT assay. RT
586 assays were performed as described previously [118] with minor modification. Briefly, after incubation of
587 the virus supernatants with RT reaction mixtures, which contained a template primer of poly (rA) (5
588 μg/ml) and oligo-dT12-18 primers (1.57 μg/ml) in 50 mM Tris, pH 7.8, 75 mM KCl, 2 mM dithiothreitol,
589 5 mM $MgCl_2$, 0.05% Nonidet P-40, and 0.25 μCi of ^{32}P-dTTP at 37°C for 3 hrs, the mixtures were
590 spotted onto filtermat B (Perkin Elmer, cat#1450-521) soaked in 0.5% (v/v) branched-polyethylenimine
591 (Merck Millipore, cat#402727). After washing the spotted filtermat with 2 x SSC buffer (300 mM NaCl
592 and 30 mM sodium citrate), levels of bound ^{32}P were measured on a Wallac BetaMax plate reader (Perkin
593 Elmer). $TCID_{50}$ of the virus stocks was determined using TZM-bl cells.
594
595 **Virus replication kinetics assays.**
596 Virus replication was monitored in SupT1 cells as previously described with minor modifications [48].
597 Briefly, SupT1 cells were incubated with pNL4-3 clones (1.0 μg/1.0 x 10^6 cells) in the presence of 700
598 μg/ml DEAE-dextran at 37°C for 15 min. Transfected cells (1.5 x 10^5 cells) were plated in 96 well flat-
599 bottom plates and incubated at 37°C in the presence of various concentrations of ARVs. For CCR5-tropic
600 viruses, we used SupT1huR5 cells, which express high levels of human CCR5. Aliquots of supernatants
601 were collected to monitor RT activity, and cells were split 1:3 every other day with fresh drug and media.
602 IC_{50} values were calculated based on RT activity at the peak of replication of each virus. To identify the
603 selected mutations in Pol/Env-coding region, genomic DNA was extracted from infected cells using
604 DNeasy Blood & Tissue mini kit (Qiagen), and then the Pol and Env-coding regions were amplified by

PrimeSTAR GXL DNA Polymerase (Takara) and sequenced (Psomagen) using previously described primers [48].

Single-round infection assays.

For cell-free infectivity assays, TZM-bl cells (1.0 x 10^4 cells) in 96-well plates were exposed to RT-normalized virus stocks produced in HeLa cells. For drug sensitivity assays, 100 $TCID_{50}$ of virus produced in 293T cells was exposed to TZM-bl cells (1.0 x 10^4 cells) in the presence of various concentrations of drugs or neutralizing antibodies. For sCD4 sensitivity assay, prior to the infection, the viruses were incubated with various concentration of sCD4 at 37°C for 0 or 2 hrs. For assays using PIs or ALLINIs, viruses were produced in the presence of serial dilutions of inhibitors as described previously [119]. Briefly, 293T cells were transfected with WT or mutant molecular clones as indicated above. 6 hrs post-transfection, 1.5 x 10^5 transfected cells were incubated with a 3-fold serial dilution of the inhibitors at 37°C for 48 hrs. Virus-containing supernatants were harvested and used to infect TZM-bl cells. At 48 hrs post-infection, luciferase activity was measured using the Britelite plus reporter gene assay system and Wallac BetaMax plate reader (Perkin Elmer).

gp120 shedding assay.

To analyze time-dependent gp120 shedding, viruses produced from HeLa cells were incubated at 37°C for 0, 1, 3, or 5 days. For the sCD4-induced gp120 shedding assay, concentrated viruses were incubated with sCD4 (0, 0.3, 1.0. 3.0, and 10 μg/ml) at 37°C for 2 hrs. Following incubation, the viruses were purified by ultracentrifugation through 20% sucrose cushions (60,000 x g) for 45 min at 4°C. The levels of virion-associated gp160, gp120, and p24 were determined by western blotting.

Western blotting.

Viral proteins were separated by SDS-PAGE and transferred to polyvinylidene disulfide (PVDF) membranes (Merck Millipore). After blocking the membranes with 5% skim milk, they were probed with

primary antibodies for 1 hr, and then incubated for 1 hr with species-specific horseradish peroxidase-conjugated secondary antibody. After the final washes, bands were detected by chemiluminescence with a Sapphire Biomolecular Imager (Azure Biosystems). Quantification was performed using ImageStudio Lite (Li-Cor Biosciences) software. The p24 protein was detected with anti-HIV-Ig at a final concentration of 5.0 µg/ml in 5% skim milk. Gp160 and gp120 were detected with the 16H3 monoclonal antibody at a final concentration of 0.5 µg/ml in 5% skim milk.

Antibody binding assay.

HEK293T cells were transfected with pBR43IeG constructs as indicated above. At 24 hrs post-transfection, the cells were detached with 5 mM EDTA/PBS, and then washed with PBS. 2.0 x 10^5 cells were incubated with the specified antibodies at a final concentration of 1.0 µg/ml at 4°C. After 1 hr incubation, the cells were washed with PBS and incubated with allophycocyanin (APC)-conjugated F(ab′)2 fragment donkey anti-human IgG antibody (Jackson ImmunoResearch Laboratories, cat# 709-136-149) at a final concentration of 62.5 µg/ml. The cells were washed with PBS and fixed with 4% paraformaldehyde (PFA, Boston Biosciences). Fixed cells were analyzed with BD LSR-II (BD Biosciences). Data were analyzed by FCS Express Cytometry Software 7 (De novo Software).

Ethics Statement.

Plasma samples were obtained prior to and after virologic failure from donors on combination ART of ritonavir (RTV)-boosted lopinavir (100 mg RTV, 400 mg LPV) plus 400 mg RAL twice a day. Samples were collected by the AIDS Clinical Trial Group (ACTG) study A5273 - a randomized, open-label, phase 3, non-inferiority study at 15 research sites in nine resource-limited countries (three sites in India and South Africa, two in Malawi and Peru, and one each in Brazil, Kenya, Tanzania, Thailand, and Zimbabwe) [5]. The primary endpoint was time to confirmed virologic failure (two measurements of HIV-1 RNA viral load >400 copies/ml). This trial was registered with ClinicalTrials.gov, NCT01352715.

Entry and exclusion criteria are listed in the protocol [5]. The study was approved by ethics committees at each site and written informed consent was obtained from each participant.

Plasma viral RNA extraction and cDNA synthesis.

Viral RNA was extracted from plasma containing 200-20,000 copies of HIV-1 RNA. Plasma was first centrifuged at 5,300 x g for 10 min at 4ºC to remove cellular debris. The supernatant was then centrifuged at 21,000 x g for 1 hr at 4ºC. Viral RNA was extracted from the viral pellet as previously described [120] and resuspended in 40 µl of RNase-free 5 mM Tris-HCl, pH 8.0. Five µl each of 10 mM dNTPs and 10 µM oligo dT were added prior to denaturing the RNA at 65ºC for 10 min. cDNA was synthesized as previously described [121] except at 50ºC for 1 hr followed by 55ºC for another hour. Two µl RNase H (2U/reaction) were added and the RNA was digested at 37ºC for 20 min.

Single-genome sequencing.

To obtain integrase PCR products from single cDNA molecules, cDNA was serially diluted to an endpoint (when approximately 30% of reactions yield PCR product). PCR master mix was prepared as previously described [121, 122] except primers targeting HIV integrase were used: Poli5 (OF) and Poli8 (OR) followed by Poli7 (IF) and Poli6 (IR) [123] in a nested PCR. PCR cycling conditions were modified by decreasing annealing temperature to 50ºC and increasing elongation time to 1 min and 30 s. To obtain *env* PCR products from single cDNA molecules, the same diluted cDNA was used but with the following primers, modified from [124]: HIVC.short.VIF1.F1 (5'-GTTTATTACAGGGACAGCAGA-3') and HIV.short OFM.R1 (5'-CAAGGCAAGCTTTATTGAGGCTTA-3'). Alternatively, E0 forward primer [125] was used. PCR cycling was performed as follows: 95ºC for 2 min and 44 cycles of 95ºC for 30 s, 57ºC for 30 s and 68ºC for 3 min – 3 min 30 s, followed by final elongation of 68ºC for 5 min. Nested PCR was performed with the following primers, modified from [126]: HIVC.short.ENVA.F2 (5'-GCATCTCCTATGGCAGGAAG-3') and HIV.short.ENVN.R2 (5'-CAATCAGGGAAGTAGCCTTG-3'). Alternatively, E00 forward primer [125] was used. PCR cycling was performed as follows: 95ºC for

683 2 min, 10 cycles 95°C for 15 s, 57°C for 30 s and 68°C for 3 min, followed by 30 cycles of 95°C for 15 s,
684 57°C for 30 s and 68°C for 2 min + 5 s per cycle, and a final elongation of 68°C for 7 min. Positive wells
685 were identified by detection using 1% agarose E-Gel™ 96-well gels (ThermoFisher Scientific) and
686 positive PCR reactions were sequenced by Sanger sequencing. For sequencing integrase: Poli7, Poli9D,
687 and O-Poli2C forward and Poli6, Poli10B and Poli3 reverse primers were used [123]. For sequencing *env*:
688 E00, For14, For15, For17, For18 and For19 forward and HIVCshort.ENVN.R2, Rev14, Rev16, Rev17,
689 and Rev18 reverse primers were used [124, 125, 127]. Additional primers used for *env* sequencing are as
690 follows:

691 For13: 5'-GAGAAAGAGCAGAAGACAGTGG-3'
692 For16: 5'-TTTAATTGTGGAGGAGAATTTTTCTA-3'
693 Rev19: 5'-ACTTTTTGACCACTTGCCACCCAT-3'
694 HIVC.REV20.SEQ: 5'-CACATGGAATTAAGCCAG-3'
695

696 **Sequence Analysis.**

697 Sanger sequencing data were analyzed using MEGA [128] to align and translate sequences. Sequences
698 were analyzed for known INSTI resistance mutations using HIV Stanford HIV Drug Resistance database:
699 https://hivdb.stanford.edu/
700

701 **Statistical analyses.**

702 Two-tailed unpaired *t*-tests and Fischer's exact tests were performed using GraphPad Prism 8 (Graphpad).
703 $*p < 0.05$, $** p < 0.01$, $*** p < 0.001$ were considered statistically significant. GraphPad Prism was also
704 used to assess statistical significance by one-way ANOVA and Tukey's multiple comparison test.
705

706 ## Acknowledgments

We thank members of the Freed laboratory for helpful discussion and critical review of the manuscript. We thank James Thomas (Leidos) for assistance with flow-cytometry analysis. We also thank Michael Bale for assistance with sequence analysis and bioinformatics support. We thank James Hoxie for providing the SupT1 huCCR5 cell line and Alan Engelman for providing BI-224436. The following reagents were obtained through the NIH AIDS Reagent Program, Division of AIDS, NIAID, NIH. Efavirenz, Emtricitabine, Nelfinavir, Maraviroc, AMD3100, T-20, Raltegravir from Merck & Company, Inc, SIM.4 from James Hildreth, sCD4 from Progenics, PGT145, PGT121 and PG16 from IAVI, 2G12 from Polymun Scientific, VRC01 from John Mascola, 447-52D from Susan Zolla-Pazner, 17b from James E. Robinson, 10E8 from Mark Connors, F105 from Marshall Posner and Lisa Cavacini, 35O22 from Jinghe Huang and Mark Connors. 16H3 from Barton F. Haynes and Hua-Xin Liao, HIV-Ig from NABI and NHLBI, pBR-NL43-IRES-eGFP-nef^{+} from Frank Kirchhoff, pK3016 from Christina Ochsenbauer and John Kappes.

Financial Disclosure Statement

Research in the Freed lab is supported by the Intramural Research Program of the Center for Cancer Research, National Cancer Institute, National Institutes of Health. YH is supported by JSPS Research Fellowship for Japanese Biomedical and Behavioral Researchers at National Institute of Health. This project has been funded in part with Federal funds from the National Cancer Institute, National Institutes of Health, under Contract number HHSN261200800001E to JWM. The content of this publication does not necessarily reflect the views of policies of the Department of Health and Human Services, nor does mention of trade names, commercial products, or organizations imply endorsement by the U.S. Government.

The National Institute of Allergy and Infectious Diseases, of the National Institutes of Health, under Award Numbers UM1AI068636, UM1AI069494, and UM1AI106701 to the AIDS Clinical Trials Group, the Pitt-Ohio State Clinical Trials Unit, and the University of Pittsburgh VSL, supported research

reported in this publication. The content is solely the responsibility of the authors and does not necessarily represent the official views of the National Institute of Allergy and Infectious Diseases or the National Institutes of Health.

Author Contributions

Conceived and designed the experiments: YH EOF. Performed the experiments: YH RVD PP JLG AW. Analyzed the data: YH RVD JLG MFK EOF. Contributed reagents/materials/analysis tools: YH RVD JLG JWM. Wrote the paper: YH JLG MFK EOF.

References

1. Kemnic TR, Gulick PG. HIV Antiretroviral Therapy: StatPearls Publishing; 2019.

2. Collier DA, Monit C, Gupta RK. The Impact of HIV-1 Drug Escape on the Global Treatment Landscape. Cell Host Microbe. 2019;26(1):48-60. Epub 2019/07/12. doi: 10.1016/j.chom.2019.06.010.

3. Perrier M, Castain L, Regad L, Todesco E, Landman R, Visseaux B, et al. HIV-1 protease, Gag and gp41 baseline substitutions associated with virological response to a PI-based regimen. Journal of Antimicrobial Chemotherapy. 2019;74(6):1679-1692. doi: 10.1093/jac/dkz043.

4. Manasa J, Varghese V, Pond SLK, Rhee SY, Tzou PL, Fessel WJ, et al. Evolution of gag and gp41 in Patients Receiving Ritonavir-Boosted Protease Inhibitors. Scientific Reports. 2017;7(1):11559. Epub 2017/09/14. doi: 10.1038/s41598-017-11893-8.

5. La Rosa AM, Harrison LJ, Taiwo B, Wallis CL, Zheng L, Kim P, et al. Raltegravir in second-line antiretroviral therapy in resource-limited settings (SELECT): a randomised, phase 3, non-inferiority study. The Lancet HIV. 2016;3(6):e247-e258. doi: 10.1016/S2352-3018(16)30011-X.

6. Hocqueloux L, Raffi F, Prazuck T, Bernard L, Sunder S, Esnault JL, et al. Dolutegravir Monotherapy Versus Dolutegravir/Abacavir/Lamivudine for Virologically Suppressed People Living with Chronic Human Immunodeficiency Virus Infection: The Randomized Noninferiority MONotherapy of TiviCAY Trial. Clinical Infectious Diseases. 2019;69(9):1498-1505. doi: 10.1093/cid/ciy1132.

758 7. Havlir DV, Hellmann NS, Petropoulos CJ, Whitcomb JM, Collier AC, Hirsch MS, et al. Drug
759 susceptibility in HIV infection after viral rebound in patients receiving indinavir-containing regimens.
760 Journal of the American Medical Association. 2000;283(2):229-234. doi: 10.1001/jama.283.2.229.

761 8. Datir R, Kemp S, Bouzidi KE, Mlchocova P, Goldstein R, Breuer J, et al. In Vivo Emergence of a
762 Novel Protease Inhibitor Resistance Signature in HIV-1 Matrix. bioRxiv. 2019:865840-865840. doi:
763 10.1101/865840.

764 9. Coetzer M, Ledingham L, Diero L, Kemboi E, Orido M, Kantor R. Gp41 and Gag amino acids
765 linked to HIV-1 protease inhibitor-based second-line failure in HIV-1 subtype A from Western Kenya.
766 Journal of the International AIDS Society. 2017;20(3). doi: 10.1002/jia2.25024.

767 10. Castain L, Perrier M, Charpentier C, Palich R, Desire N, Wirden M, et al. New mechanisms of
768 resistance in virological failure to protease inhibitors: Selection of non-described protease, Gag and Gp41
769 mutations. Journal of Antimicrobial Chemotherapy. 2019;74(7):2019-2023. doi: 10.1093/jac/dkz151.

770 11. Dicker IB, Samanta HK, Li Z, Hong Y, Tian Y, Banville J, et al. Changes to the HIV long
771 terminal repeat and to HIV integrase differentially impact HIV integrase assembly, activity, and the
772 binding of strand transfer inhibitors. Journal of Biological Chemistry. 2007;282(43):31186-31196. doi:
773 10.1074/jbc.M704935200.

774 12. Malet I, Subra F, Charpentier C, Collin G, Descamps D, Calvez V, et al. Mutations located
775 outside the integrase gene can confer resistance to HIV-1 integrase strand transfer inhibitors. mBio.
776 2017;8(5). doi: 10.1128/mBio.00922-17.

777 13. Rabi SA, Laird GM, Durand CM, Laskey S, Shan L, Bailey JR, et al. Multi-step inhibition
778 explains HIV-1 protease inhibitor pharmacodynamics and resistance. Journal of Clinical Investigation.
779 2013;123(9):3848-3860. doi: 10.1172/JCI67399.

780 14. Fun A, Wensing AM, Verheyen J, Nijhuis M. Human Immunodeficiency Virus Gag and protease:
781 partners in resistance. Retrovirology. 2012;9:63. Epub 2012/08/06. doi: 10.1186/1742-4690-9-63.

782 15. Checkley MA, Luttge BG, Freed EO. HIV-1 envelope glycoprotein biosynthesis, trafficking, and
783 incorporation. Journal of Molecular Biology. 2011;410(4):582-608. doi: 10.1016/j.jmb.2011.04.042.

784 16. Wilen CB, Tilton JC, Doms RW. HIV: cell binding and entry. Cold Spring Harbor perspectives in
785 medicine. 2012;2(8). Epub 2012/08/01. doi: 10.1101/cshperspect.a006866.

786 17. McCoy LE, Burton DR. Identification and specificity of broadly neutralizing antibodies against
787 HIV. Immunological Reviews. 2017;275(1):11-20. doi: 10.1111/imr.12484.

788 18. Munro JB, Gorman J, Ma X, Zhou Z, Arthos J, Burton DR, et al. Conformational dynamics of
789 single HIV-1 envelope trimers on the surface of native virions. Science. 2014;346(6210):759-763. doi:
790 10.1126/science.1254426.

791 19. Herschhorn A, Ma X, Gu C, Ventura JD, Castillo-Menendez L, Melillo B, et al. Release of
792 GP120 restraints leads to an entry-competent intermediate state of the HIV-1 envelope glycoproteins.
793 mBio. 2016;7(5). doi: 10.1128/mBio.01598-16.

794 20. Hübner W, McNerney GP, Chen P, Dale BM, Gordon RE, Chuang FY, et al. Quantitative 3D
795 video microscopy of HIV transfer across T cell virological synapses. Science. 2009;323(5922):1743-
796 1747. doi: 10.1126/science.1167525.

797 21. Rudnicka D, Feldmann J, Porrot F, Wietgrefe S, Guadagnini S, Prévost MC, et al. Simultaneous
798 cell-to-cell transmission of human immunodeficiency virus to multiple targets through polysynapses.
799 Journal of Virology. 2009;83(12):6234-6246. Epub 2009/04/15. doi: 10.1128/JVI.00282-09.

800 22. Sherer NM, Lehmann MJ, Jimenez-Soto LF, Ingmundson A, Horner SM, Cicchetti G, et al.
801 Visualization of retroviral replication in living cells reveals budding into multivesicular bodies. Traffic.
802 2003;4(11):785-801. doi: 10.1034/j.1600-0854.2003.00135.x.

803 23. Gousset K, Ablan SD, Coren LV, Ono A, Soheilian F, Nagashima K, et al. Real-time
804 visualization of HIV-1 GAG trafficking in infected macrophages. PLoS Pathogens. 2008;4(3):e1000015.
805 Epub 2008/03/07. doi: 10.1371/journal.ppat.1000015.

806 24. Jolly C. T cell polarization at the virological synapse. Viruses. 2010;2(6):1261-1278. Epub
807 2010/05/31. doi: 10.3390/v2061261.

808 25. Jolly C, Kashefi K, Hollinshead M, Sattentau QJ. HIV-1 Cell to Cell Transfer across an Env-
809 induced, Actin-dependent Synapse. Journal of Experimental Medicine. 2004;199(2):283-293. doi:
810 10.1084/jem.20030648.

811 26. Jolly C, Mitar I, Sattentau QJ. Adhesion molecule interactions facilitate human
812 immunodeficiency virus type 1-induced virological synapse formation between T cells. Journal of
813 Virology. 2007;81(24):13916-13921. Epub 2007/10/03. doi: 10.1128/JVI.01585-07.

814 27. Dimitrov DS, Willey RL, Sato H, Chang LJ, Blumenthal R, Martin MA. Quantitation of human
815 immunodeficiency virus type 1 infection kinetics. Journal of Virology. 1993;67(4):2182-2190.

816 28. Sato H, Orenstein J, Dimitrov D, Martin M. Cell-to-cell spread of HIV-1 occurs within minutes
817 and may not involve the participation of virus particles. Virology. 1992;186(2):712-724. doi:
818 10.1016/0042-6822(92)90038-q.

29. Sourisseau M, Sol-Foulon N, Porrot F, Blanchet F, Schwartz O. Inefficient human immunodeficiency virus replication in mobile lymphocytes. Journal of Virology. 2007;81(2):1000-1012. Epub 2006/11/01. doi: 10.1128/JVI.01629-06.

30. Del Portillo A, Tripodi J, Najfeld V, Wodarz D, Levy DN, Chen BK. Multiploid Inheritance of HIV-1 during Cell-to-Cell Infection. Journal of Virology. 2011;85(14):7169-7176. doi: 10.1128/jvi.00231-11.

31. Russell RA, Martin N, Mitar I, Jones E, Sattentau QJ. Multiple proviral integration events after virological synapse-mediated HIV-1 spread. Virology. 2013;443(1):143-149. Epub 2013/05/28. doi: 10.1016/j.virol.2013.05.005.

32. Sigal A, Kim JT, Balazs AB, Dekel E, Mayo A, Milo R, et al. Cell-to-cell spread of HIV permits ongoing replication despite antiretroviral therapy. Nature. 2011;477(7362):95-99. doi: 10.1038/nature10347.

33. Zhong P, Agosto LM, Ilinskaya A, Dorjbal B, Truong R, Derse D, et al. Cell-to-Cell Transmission Can Overcome Multiple Donor and Target Cell Barriers Imposed on Cell-Free HIV. PLoS One. 2013;8(1). doi: 10.1371/journal.pone.0053138.

34. Agosto LM, Zhong P, Munro J, Mothes W. Highly Active Antiretroviral Therapies Are Effective against HIV-1 Cell-to-Cell Transmission. PLoS Pathogens. 2014;10(2). doi: 10.1371/journal.ppat.1003982.

35. Bastarache SM, Mesplède T, Donahue DA, Sloan RD, Wainberg MA. Fitness impaired drug resistant HIV-1 is not compromised in cell-to-cell transmission or establishment of and reactivation from latency. Viruses. 2014;6(9):3487-3499. doi: 10.3390/v6093487.

36. Boullé M, Müller TG, Dähling S, Ganga Y, Jackson L, Mahamed D, et al. HIV Cell-to-Cell Spread Results in Earlier Onset of Viral Gene Expression by Multiple Infections per Cell. PLoS Pathogens. 2016;12(11):e1005964-e1005964. doi: 10.1371/journal.ppat.1005964.

37. Dufloo J, Bruel T, Schwartz O. HIV-1 cell-to-cell transmission and broadly neutralizing antibodies. Retrovirology. 2018;15:51-51. doi: 10.1186/s12977-018-0434-1.

38. Titanji BK, Aasa-Chapman M, Pillay D, Jolly C. Protease inhibitors effectively block cell-to-cell spread of HIV-1 between T cells. Retrovirology. 2013;10:161-161. doi: 10.1186/1742-4690-10-161.

39. Murooka TT, Deruaz M, Marangoni F, Vrbanac VD, Seung E, von Andrian UH, et al. HIV-infected T cells are migratory vehicles for viral dissemination. Nature. 2012;490(7419):283-287. Epub 2012/08/01. doi: 10.1038/nature11398.

850 40. Law KM, Komarova NL, Yewdall AW, Lee RK, Herrera OL, Wodarz D, et al. In Vivo HIV-1
851 Cell-to-Cell Transmission Promotes Multicopy Micro-compartmentalized Infection. Cell Reports.
852 2016;15(12):2771-2783. Epub 2016/06/09. doi: 10.1016/j.celrep.2016.05.059.

853 41. Kieffer C, Ladinsky MS, Ninh A, Galimidi RP, Bjorkman PJ. Longitudinal imaging of HIV-1
854 spread in humanized mice with parallel 3D immunofluorescence and electron tomography. Elife. 2017;6.
855 Epub 2017/02/15. doi: 10.7554/eLife.23282.

856 42. Ladinsky MS, Khamaikawin W, Jung Y, Lin S, Lam J, An DS, et al. Mechanisms of virus
857 dissemination in bone marrow of HIV-1-infected humanized BLT mice. Elife. 2019;8. Epub 2019/10/28.
858 doi: 10.7554/eLife.46916.

859 43. Ladinsky MS, Kieffer C, Olson G, Deruaz M, Vrbanac V, Tager AM, et al. Electron tomography
860 of HIV-1 infection in gut-associated lymphoid tissue. PLoS Pathogens. 2014;10(1):e1003899. Epub
861 2014/01/30. doi: 10.1371/journal.ppat.1003899.

862 44. Gratton S, Cheynier R, Dumaurier MJ, Oksenhendler E, Wain-Hobson S. Highly restricted spread
863 of HIV-1 and multiply infected cells within splenic germinal centers. Proceedings of the National
864 Academy of Sciences of the United States of America. 2000;97(26):14566-14571. doi:
865 10.1073/pnas.97.26.14566.

866 45. Jung A, Maier R, Vartanian JP, Bocharov G, Jung V, Fischer U, et al. Recombination: Multiply
867 infected spleen cells in HIV patients. Nature. 2002;418(6894):144. doi: 10.1038/418144a.

868 46. Suspène R, Meyerhans A. Quantification of unintegrated HIV-1 DNA at the single cell level in
869 vivo. PLoS One. 2012;7(5):e36246. Epub 2012/05/04. doi: 10.1371/journal.pone.0036246.

870 47. Josefsson L, Palmer S, Faria NR, Lemey P, Casazza J, Ambrozak D, et al. Single cell analysis of
871 lymph node tissue from HIV-1 infected patients reveals that the majority of CD4+ T-cells contain one
872 HIV-1 DNA molecule. PLoS Pathogens. 2013;9(6):e1003432. Epub 2013/06/20. doi:
873 10.1371/journal.ppat.1003432.

874 48. Van Duyne R, Kuo LS, Pham P, Fujii K, Freed EO. Mutations in the HIV-1 envelope
875 glycoprotein can broadly rescue blocks at multiple steps in the virus replication cycle. Proceedings of the
876 National Academy of Sciences of the United States of America. 2019;116(18):9040-9049. doi:
877 10.1073/pnas.1820333116.

878 49. Fujii K, Munshi UM, Ablan SD, Demirov DG, Soheilian F, Nagashima K, et al. Functional role
879 of Alix in HIV-1 replication. Virology. 2009;391(2):284-292. doi: 10.1016/j.virol.2009.06.016.

880 50. Finzi A, Xiang SH, Pacheco B, Wang L, Haight J, Kassa A, et al. Topological Layers in the HIV-
881 1 gp120 Inner Domain Regulate gp41 Interaction and CD4-Triggered Conformational Transitions.
882 Molecular Cell. 2010;37(5):656-667. doi: 10.1016/j.molcel.2010.02.012.

883 51. Korkut A, Hendrickson WA. Structural Plasticity and Conformational Transitions of HIV
884 Envelope Glycoprotein gp120. PLoS One. 2012;7(12):e52170-e52170. doi:
885 10.1371/journal.pone.0052170.

886 52. Pacheco B, Alsahafi N, Debbeche O, Prévost J, Ding S, Chapleau J-P, et al. Residues in the gp41
887 Ectodomain Regulate HIV-1 Envelope Glycoprotein Conformational Transitions Induced by gp120-
888 Directed Inhibitors. Journal of Virology. 2017;91(5). doi: 10.1128/jvi.02219-16.

889 53. Wrin T, Loh TP, Vennari JC, Schuitemaker H, Nunberg JH. Adaptation to persistent growth in
890 the H9 cell line renders a primary isolate of human immunodeficiency virus type 1 sensitive to
891 neutralization by vaccine sera. Journal of Virology. 1995;69(1):39-48. doi: doi:10.1128/JVI.69.1.39-
892 48.1995.

893 54. Pugach P, Kuhmann SE, Taylor J, Marozsan AJ, Snyder A, Ketas T, et al. The prolonged culture
894 of human immunodeficiency virus type 1 in primary lymphocytes increases its sensitivity to
895 neutralization by soluble CD4. Virology. 2004;321(1):8-22. doi: 10.1016/j.virol.2003.12.012.

896 55. Moore JP, McKeating JA, Huang YX, Ashkenazi A, Ho DD. Virions of primary human
897 immunodeficiency virus type 1 isolates resistant to soluble CD4 (sCD4) neutralization differ in sCD4
898 binding and glycoprotein gp120 retention from sCD4-sensitive isolates. Journal of virology.
899 1992;66(1):235-243. doi: 10.1128/JVI.66.1.235-243.1992. .

900 56. Moore J, McKeating J, Weiss R, Sattentau Q. Dissociation of gp120 from HIV-1 virions induced
901 by soluble CD4. Science. 1990;250(4984):1139-1142. doi: 10.1126/science.2251501.

902 57. Hammonds J, Chen X, Ding L, Fouts T, De Vico A, Zur Megede J, et al. Gp120 stability on HIV-
903 1 virions and Gag-Env pseudovirions is enhanced by an uncleaved Gag core. Virology. 2003;314(2):636-
904 649. doi: 10.1016/S0042-6822(03)00467-7.

905 58. Engelman AN. Multifaceted HIV integrase functionalities and therapeutic strategies for their
906 inhibition. Journal of Biological Chemistry. 2019;294(41):15137-15157. Epub 2019/08/29. doi:
907 10.1074/jbc.REV119.006901.

908 59. Martin N, Welsch S, Jolly C, Briggs JA, Vaux D, Sattentau QJ. Virological synapse-mediated
909 spread of human immunodeficiency virus type 1 between T cells is sensitive to entry inhibition. Journal
910 of Virology. 2010;84(7):3516-3527. Epub 2010/01/20. doi: 10.1128/JVI.02651-09.

911 60. Abela IA, Berlinger L, Schanz M, Reynell L, Günthard HF, Rusert P, et al. Cell-cell transmission
912 enables HIV-1 to evade inhibition by potent CD4bs directed antibodies. PLoS Pathogens. 2012;8(4). doi:
913 10.1371/journal.ppat.1002634.

914 61. Yoshimura K, Harada S, Boonchawalit S, Kawanami Y, Matsushita S. Impact of maraviroc-
915 resistant and low-CCR5-adapted mutations induced by in vitro passage on sensitivity to anti-envelope
916 neutralizing antibodies. Journal of General Virology. 2014. doi: 10.1099/vir.0.062885-0.

917 62. Keller PW, Morrison O, Vassell R, Weiss CD. HIV-1 gp41 Residues Modulate CD4-Induced
918 Conformational Changes in the Envelope Glycoprotein and Evolution of a Relaxed Conformation of
919 gp120. Journal of Virology. 2018;92(16). doi: 10.1128/jvi.00583-18.

920 63. Hikichi Y, Yokoyama M, Takemura T, Fujino M, Kumakura S, Maeda Y, et al. Increased HIV-1
921 sensitivity to neutralizing antibodies by mutations in the Env V3-coding region for resistance to CXCR4
922 antagonists. Journal of General Virology. 2016;97(9):2427-2440. doi: 10.1099/jgv.0.000536.

923 64. Berro R, Sanders RW, Lu M, Klasse PJ, Moore JP. Two HIV-1 variants resistant to small
924 molecule CCR5 inhibitors differ in how they use CCR5 for entry. PLoS Pathogens. 2009;5(8):e1000548.
925 Epub 2009/08/14. doi: 10.1371/journal.ppat.1000548.

926 65. Melikian GL, Rhee SY, Varghese V, Porter D, White K, Taylor J, et al. Non-nucleoside reverse
927 transcriptase inhibitor (NNRTI) cross-resistance: implications for preclinical evaluation of novel NNRTIs
928 and clinical genotypic resistance testing. Journal of Antimicrobial Chemotherapy. 2014;69(1):12-20.
929 Epub 2013/08/09. doi: 10.1093/jac/dkt316.

930 66. Wang Q, Liu L, Ren W, Gettie A, Wang H, Liang Q, et al. A Single Substitution in gp41
931 Modulates the Neutralization Profile of SHIV during In Vivo Adaptation. Cell Reports. 2019;27(9):2593-
932 2607.e2595. doi: 10.1016/j.celrep.2019.04.108.

933 67. Ma X, Lu M, Gorman J, Terry DS, Hong X, Zhou Z, et al. HIV-1 Env trimer opens through an
934 asymmetric intermediate in which individual protomers adopt distinct conformations. Elife. 2018;7. Epub
935 2018/03/21. doi: 10.7554/eLife.34271.

936 68. Buchacher A, Predl R, Strutzenberger K, Steinfellner W, Trkola A, Purtscher M, et al. Generation
937 of human monoclonal antibodies against HIV-1 proteins; electrofusion and Epstein-Barr virus
938 transformation for peripheral blood lymphocyte immortalization. AIDS research and human retroviruses.
939 1994;10(4):359-369. doi: 10.1089/aid.1994.10.359.

940 69. Walker LM, Huber M, Doores KJ, Falkowska E, Pejchal R, Julien JP, et al. Broad neutralization
941 coverage of HIV by multiple highly potent antibodies. Nature. 2011;477(7365):466-470. doi:
942 10.1038/nature10373.

943 70. Walker LM, Phogat SK, Chan-Hui PY, Wagner D, Phung P, Goss JL, et al. Broad and potent
944 neutralizing antibodies from an African donor reveal a new HIV-1 vaccine target. Science.
945 2009;326(5950):285-289. Epub 2009/09/03. doi: 10.1126/science.1178746.

946 71. Wu X, Yang ZY, Li Y, Hogerkorp CM, Schief WR, Seaman MS, et al. Rational design of
947 envelope identifies broadly neutralizing human monoclonal antibodies to HIV-1. Science.
948 2010;329(5993):856-861. Epub 2010/07/08. doi: 10.1126/science.1187659.

949 72. Huang J, Kang BH, Pancera M, Lee JH, Tong T, Feng Y, et al. Broad and potent HIV-1
950 neutralization by a human antibody that binds the gp41-gp120 interface. Nature. 2014;515(7525):138-
951 142. Epub 2014/09/03. doi: 10.1038/nature13601.

952 73. Cavacini LA, Emes CL, Power J, Buchbinder A, Zolla-Pazner S, Posner MR. Human monoclonal
953 antibodies to the V3 loop of HIV-1 gp120 mediate variable and distinct effects on binding and viral
954 neutralization by a human monoclonal antibody to the CD4 binding site. Journal of Acquired Immune
955 Deficiency Syndromes. 1993;6(4):353-358.

956 74. Gorny MK, Conley AJ, Karwowska S, Buchbinder A, Xu JY, Emini EA, et al. Neutralization of
957 diverse human immunodeficiency virus type 1 variants by an anti-V3 human monoclonal antibody.
958 Journal of Virology. 1992;66(12):7538-7542. doi: 10.1128/JVI.66.12.7538-7542.1992.

959 75. Huang J, Ofek G, Laub L, Louder MK, Doria-Rose NA, Longo NS, et al. Broad and potent
960 neutralization of HIV-1 by a gp41-specific human antibody. Nature. 2012;491(7424):406-412. Epub
961 2012/09/18. doi: 10.1038/nature11544.

962 76. Thali M, Moore JP, Furman C, Charles M, Ho DD, Robinson J, et al. Characterization of
963 conserved human immunodeficiency virus type 1 gp120 neutralization epitopes exposed upon gp120-
964 CD4 binding. Journal of Virology. 1993;67(7):3978-3988.

965 77. McCallus DE, Ugen KE, Sato AI, Williams WV, Weiner DB. Construction of a recombinant
966 bacterial human CD4 expression system producing a bioactive CD4 molecule. Viral Immunology.
967 1992;5(2):163-172. doi: 10.1089/vim.1992.5.163.

968 78. De Clercq E, Yamamoto N, Pauwels R, Balzarini J, Witvrouw M, De Vreese K, et al. Highly
969 potent and selective inhibition of human immunodeficiency virus by the bicyclam derivative JM3100.
970 Antimicrobial Agents and Chemotherapy. 1994;38(4):668-674. doi: 10.1128/aac.38.4.668.

971 79. Freed EO, Englund G, Martin MA. Role of the basic domain of human immunodeficiency virus
972 type 1 matrix in macrophage infection. Journal of virology. 1995;69(6):3949-3954. doi:
973 10.1128/jvi.69.6.3949-3954.1995.

974 80. Parrish NF, Gao F, Li H, Giorgi EE, Barbian HJ, Parrish EH, et al. Phenotypic properties of
975 transmitted founder HIV-1. Proceedings of the National Academy of Sciences of the United States of
976 America. 2013;110(17):6626-6633. doi: 10.1073/pnas.1304288110.

977 81. Moore PL, Gray ES, Choge IA, Ranchobe N, Mlisana K, Abdool Karim SS, et al. The c3-v4
978 region is a major target of autologous neutralizing antibodies in human immunodeficiency virus type 1
979 subtype C infection. Journal of Virology. 2008;82(4):1860-1869. Epub 2007/12/05. doi:
980 10.1128/JVI.02187-07.

981 82. Wibmer CK, Bhiman JN, Gray ES, Tumba N, Abdool Karim SS, Williamson C, et al. Viral
982 escape from HIV-1 neutralizing antibodies drives increased plasma neutralization breadth through
983 sequential recognition of multiple epitopes and immunotypes. PLoS Pathogens. 2013;9(10):e1003738.
984 Epub 2013/10/31. doi: 10.1371/journal.ppat.1003738.

985 83. Durham ND, Yewdall AW, Chen P, Lee R, Zony C, Robinson JE, et al. Neutralization resistance
986 of virological synapse-mediated HIV-1 Infection is regulated by the gp41 cytoplasmic tail. Journal of
987 Virology. 2012;86(14):7484-7495. Epub 2012/05/02. doi: 10.1128/JVI.00230-12.

988 84. Reh L, Magnus C, Schanz M, Weber J, Uhr T, Rusert P, et al. Capacity of Broadly Neutralizing
989 Antibodies to Inhibit HIV-1 Cell-Cell Transmission Is Strain- and Epitope-Dependent. PLoS Pathogens.
990 2015;11(7):e1004966. Epub 2015/07/09. doi: 10.1371/journal.ppat.1004966.

991 85. Nameki D, Kodama E, Ikeuchi M, Mabuchi N, Otaka A, Tamamura H, et al. Mutations
992 conferring resistance to human immunodeficiency virus type 1 fusion inhibitors are restricted by gp41 and
993 Rev-responsive element functions. Journal of Virology. 2005;79(2):764-770. doi: 10.1128/JVI.79.2.764-
994 770.2005.

995 86. Collier D, Iwuji C, Derache A, de Oliveira T, Okesola N, Calmy A, et al. Virological Outcomes
996 of Second-line Protease Inhibitor-Based Treatment for Human Immunodeficiency Virus Type 1 in a
997 High-Prevalence Rural South African Setting: A Competing-Risks Prospective Cohort Analysis. Clinical
998 Infectious Diseases. 2017;64(8):1006-1016. doi: 10.1093/cid/cix015.

999 87. Gallego O, de Mendoza C, Pérez-Elías MJ, Guardiola JM, Pedreira J, Dalmau D, et al. Drug
1000 resistance in patients experiencing early virological failure under a triple combination including indinavir.
1001 AIDS. 2001;15(13):1701-1706. doi: 10.1097/00002030-200109070-00014.

1002 88. Hosseinipour MC, Gupta RK, Van Zyl G, Eron JJ, Nachega JB. Emergence of HIV drug
1003 resistance during first- and second-line antiretroviral therapy in resource-limited settings. The Journal of
1004 Infectious Diseases. 2013;207 Suppl 2:S49-56. doi: 10.1093/infdis/jit107.

1005 89. Pulido F, Arribas J, Hill A, Moecklinghoff C. No evidence for evolution of protease inhibitor
1006 resistance from standard genotyping, after three years of treatment with darunavir/ritonavir, with or

without nucleoside analogues. AIDS research and human retroviruses. 2012;28(10):1167-1169. Epub 2012/04/20. doi: 10.1089/AID.2011.0256.

90. Court R, Gordon M, Cohen K, Stewart A, Gosnell B, Wiesner L, et al. Random lopinavir concentrations predict resistance on lopinavir-based antiretroviral therapy. International Journal of Antimicrobial Agents. 2016;48(2):158-162. Epub 2016/06/09. doi: 10.1016/j.ijantimicag.2016.04.030.

91. van Zyl GU, van Mens TE, McIlleron H, Zeier M, Nachega JB, Decloedt E, et al. Low lopinavir plasma or hair concentrations explain second-line protease inhibitor failures in a resource-limited setting. Journal of Acquired Immune Deficiency Syndromes. 2011;56(4):333-339. doi: 10.1097/QAI.0b013e31820dc0cc.

92. Murakami T, Ablan S, Freed EO, Tanaka Y. Regulation of human immunodeficiency virus type 1 Env-mediated membrane fusion by viral protease activity. Journal of Virology. 2004;78(2):1026-1031. doi: 10.1128/jvi.78.2.1026-1031.2004.

93. Wyma DJ, Jiang J, Shi J, Zhou J, Lineberger JE, Miller MD, et al. Coupling of human immunodeficiency virus type 1 fusion to virion maturation: a novel role of the gp41 cytoplasmic tail. Journal of Virology. 2004;78(7):3429-3435. doi: 10.1128/jvi.78.7.3429-3435.2004.

94. Wijting IEA, Lungu C, Rijnders BJA, van der Ende ME, Pham HT, Mesplede T, et al. HIV-1 Resistance Dynamics in Patients With Virologic Failure to Dolutegravir Maintenance Monotherapy. The Journal of Infectious Diseases. 2018;218(5):688-697. doi: 10.1093/infdis/jiy176.

95. Ozorowski G, Pallesen J, de Val N, Lyumkis D, Cottrell CA, Torres JL, et al. Open and closed structures reveal allostery and pliability in the HIV-1 envelope spike. Nature. 2017;547(7663):360-363. Epub 2017/07/12. doi: 10.1038/nature23010.

96. Stewart-Jones GB, Soto C, Lemmin T, Chuang GY, Druz A, Kong R, et al. Trimeric HIV-1-Env Structures Define Glycan Shields from Clades A, B, and G. Cell. 2016;165(4):813-826. Epub 2016/04/21. doi: 10.1016/j.cell.2016.04.010.

97. Drummer HE, Hill MK, Maerz AL, Wood S, Ramsland PA, Mak J, et al. Allosteric modulation of the HIV-1 gp120-gp41 association site by adjacent gp120 variable region 1 (V1) N-glycans linked to neutralization sensitivity. PLoS Pathogens. 2013;9(4):e1003218. Epub 2013/04/04. doi: 10.1371/journal.ppat.1003218.

98. Narasimhulu VGS, Bellamy-McIntyre AK, Laumaea AE, Lay CS, Harrison DN, King HAD, et al. Distinct functions for the membrane-proximal ectodomain region (MPER) of HIV-1 gp41 in cell-free and cell-cell viral transmission and cell-cell fusion. Journal of Biological Chemistry. 2018;293(16):6099-6120. Epub 2018/03/01. doi: 10.1074/jbc.RA117.000537.

1039 99. Cao J, Bergeron L, Helseth E, Thali M, Repke H, Sodroski J. Effects of amino acid changes in the
1040 extracellular domain of the human immunodeficiency virus type 1 gp41 envelope glycoprotein. Journal of
1041 Virology. 1993;67(5):2747-2755.

1042 100. Diaz-Aguilar B, Dewispelaere K, Yi HA, Jacobs A. Significant differences in cell-cell fusion and
1043 viral entry between strains revealed by scanning mutagenesis of the C-heptad repeat of HIV gp41.
1044 Biochemistry. 2013;52(20):3552-3563. Epub 2013/05/07. doi: 10.1021/bi400201h.

1045 101. Kahle KM, Steger HK, Root MJ. Asymmetric deactivation of HIV-1 gp41 following fusion
1046 inhibitor binding. PLoS Pathogens. 2009;5(11):e1000674. Epub 2009/11/26. doi:
1047 10.1371/journal.ppat.1000674.

1048 102. Roy NH, Lambelé M, Chan J, Symeonides M, Thali M. Ezrin is a component of the HIV-1
1049 virological presynapse and contributes to the inhibition of cell-cell fusion. Journal of Virology.
1050 2014;88(13):7645-7658. Epub 2014/04/23. doi: 10.1128/JVI.00550-14.

1051 103. Symeonides M, Murooka TT, Bellfy LN, Roy NH, Mempel TR, Thali M. HIV-1-Induced Small
1052 T Cell Syncytia Can Transfer Virus Particles to Target Cells through Transient Contacts. Viruses.
1053 2015;7(12):6590-6603. Epub 2015/12/12. doi: 10.3390/v7122959.

1054 104. Compton AA, Schwartz O. They Might Be Giants: Does Syncytium Formation Sink or Spread
1055 HIV Infection? PLoS Pathogens. 2017;13(2):e1006099. Epub 2017/02/02. doi:
1056 10.1371/journal.ppat.1006099.

1057 105. Das AT, Land A, Braakman I, Klaver B, Berkhout B. HIV-1 evolves into a nonsyncytium-
1058 inducing virus upon prolonged culture in vitro. Virology. 1999;263(1):55-69. doi:
1059 10.1006/viro.1999.9898.

1060 106. Das AT, van Dam AP, Klaver B, Berkhout B. Improved envelope function selected by long-term
1061 cultivation of a translation-impaired HIV-1 mutant. Virology. 1998;244(2):552-562. doi:
1062 10.1006/viro.1998.9124.

1063 107. Sylwester A, Murphy S, Shutt D, Soll DR. HIV-induced T cell syncytia are self-perpetuating and
1064 the primary cause of T cell death in culture. Journal of Immunology. 1997;158(8):3996-4007.

1065 108. Van Rompay KKA, Hassounah S, Keele BF, Lifson JD, Ardeshir A, Watanabe J, et al.
1066 Dolutegravir Monotherapy of Simian Immunodeficiency Virus-Infected Macaques Selects for Several
1067 Patterns of Resistance Mutations with Variable Virological Outcomes. Journal of Virology. 2019;93(2).
1068 Epub 2019/01/04. doi: 10.1128/JVI.01189-18.

109. Wijting I, Rutsaert SL, Rokx C, Burger DM, Verbon A, van Kampen J, et al. Predictors of virological failure in HIV-1-infected patients switching to dolutegravir maintenance monotherapy. HIV Medicine. 2019;20(1):63-68. Epub 2018/09/30. doi: 10.1111/hiv.12675.

110. Anstett K, Brenner B, Mesplede T, Wainberg MA. HIV drug resistance against strand transfer integrase inhibitors. Retrovirology. 2017;14(1):36. Epub 2017/06/05. doi: 10.1186/s12977-017-0360-7.

111. Platt EJ, Wehrly K, Kuhmann SE, Chesebro B, Kabat D. Effects of CCR5 and CD4 Cell Surface Concentrations on Infections by Macrophagetropic Isolates of Human Immunodeficiency Virus Type 1. Journal of Virology. 1998;72(4):2855-2864. doi: 10.1128/jvi.72.4.2855-2864.1998.

112. Means RE, Matthews T, Hoxie JA, Malim MH, Kodama T, Desrosiers RC. Ability of the V3 loop of simian immunodeficiency virus to serve as a target for antibody-mediated neutralization: correlation of neutralization sensitivity, growth in macrophages, and decreased dependence on CD4. Journal of Virology. 2001;75(8):3903-3915. doi: 10.1128/JVI.75.8.3903-3915.2001.

113. Gao F, Scearce RM, Alam SM, Hora B, Xia S, Hohm JE, et al. Cross-reactive monoclonal antibodies to multiple HIV-1 subtype and SIVcpz envelope glycoproteins. Virology. 2009;394(1):91-98. Epub 2009/09/09. doi: 10.1016/j.virol.2009.07.041.

114. Adachi A, Gendelman HE, Koenig S, Folks T, Willey R, Rabson A, et al. Production of acquired immunodeficiency syndrome-associated retrovirus in human and nonhuman cells transfected with an infectious molecular clone. Journal of Virology. 1986;59(2):284-291. doi: 10.1128/jvi.59.2.284-291.1986.

115. Schindler M, Münch J, Kirchhoff F. Human immunodeficiency virus type 1 inhibits DNA damage-triggered apoptosis by a Nef-independent mechanism. Journal of Virology. 2005;79(9):5489-5498. doi: 10.1128/JVI.79.9.5489-5498.2005.

116. Schindler M, Würfl S, Benaroch P, Greenough TC, Daniels R, Easterbrook P, et al. Down-modulation of mature major histocompatibility complex class II and up-regulation of invariant chain cell surface expression are well-conserved functions of human and simian immunodeficiency virus nef alleles. Journal of Virology. 2003;77(19):10548-10556. doi: 10.1128/jvi.77.19.10548-10556.2003.

117. Freed EO, Delwart EL, Buchschacher GL, Panganiban AT. A mutation in the human immunodeficiency virus type 1 transmembrane glycoprotein gp41 dominantly interferes with fusion and infectivity. Proceedings of the National Academy of Sciences of the United States of America. 1992;89(1):70-74. doi: 10.1073/pnas.89.1.70.

118. Willey RL, Smith DH, Lasky LA, Theodore TS, Earl PL, Moss B, et al. In vitro mutagenesis identifies a region within the envelope gene of the human immunodeficiency virus that is critical for infectivity. Journal of Virology. 1988;62(1):139-147. doi: 10.1128/JVI.62.1.139-147.1988.

1101 119. Urano E, Timilsina U, Kaplan JA, Ablan S, Ghimire D, Pham P, et al. Resistance to Second-
1102 Generation HIV-1 Maturation Inhibitors. Journal of Virology. 2019;93(6). Epub 2018/12/21. doi:
1103 10.1128/JVI.02017-18.

1104 120. Palmer S, Kearney M, Maldarelli F, Halvas EK, Bixby CJ, Bazmi H, et al. Multiple, linked
1105 human immunodeficiency virus type 1 drug resistance mutations in treatment-experienced patients are
1106 missed by standard genotype analysis. Journal of Clinical Microbiology. 2005;43(1):406-413. doi:
1107 10.1128/JCM.43.1.406-413.2005.

1108 121. Wiegand A, Spindler J, Hong FF, Shao W, Cyktor JC, Cillo AR, et al. Single-cell analysis of
1109 HIV-1 transcriptional activity reveals expression of proviruses in expanded clones during ART.
1110 Proceedings of the National Academy of Sciences of the United States of America. 2017;114(18):E3659-
1111 E3668. Epub 2017/04/17. doi: 10.1073/pnas.1617961114.

1112 122. Kearney M, Palmer S, Maldarelli F, Shao W, Polis MA, Mican J, et al. Frequent polymorphism at
1113 drug resistance sites in HIV-1 protease and reverse transcriptase. AIDS. 2008;22(4):497-501. doi:
1114 10.1097/QAD.0b013e3282f29478.

1115 123. Swanson P, Devare SG, Hackett J. Molecular characterization of 39 HIV isolates representing
1116 group M (subtypes A-G) and group O: sequence analysis of gag p24, pol integrase, and env gp41. AIDS
1117 research and human retroviruses. 2003;19(7):625-629. doi: 10.1089/088922203322231003.

1118 124. Salazar-Gonzalez JF, Salazar MG, Keele BF, Learn GH, Giorgi EE, Li H, et al. Genetic identity,
1119 biological phenotype, and evolutionary pathways of transmitted/founder viruses in acute and early HIV-1
1120 infection. Journal of Experimental Medicine. 2009;206(6):1273-1289. Epub 2009/06/01. doi:
1121 10.1084/jem.20090378.

1122 125. Myers G KB, Hahn BH, Jeang K-T, Mellors JW, McCutchan FE, Henderson LE and Pavlakis
1123 GN. Human Retroviruses and AIDS 1995: A Compilation and Analysis of Nucleic Acid and Amino Acid
1124 Sequences. Theoretical Biology and Biophysics Group, Los Alamos National Laboratory, Los Alamos.
1125 1995.

1126 126. Salazar-Gonzalez JF, Bailes E, Pham KT, Salazar MG, Guffey MB, Keele BF, et al. Deciphering
1127 human immunodeficiency virus type 1 transmission and early envelope diversification by single-genome
1128 amplification and sequencing. Journal of Virology. 2008;82(8):3952-3970. Epub 2008/02/06. doi:
1129 10.1128/JVI.02660-07.

1130 127. Patro SC, Brandt LD, Bale MJ, Halvas EK, Joseph KW, Shao W, et al. Combined HIV-1
1131 sequence and integration site analysis informs viral dynamics and allows reconstruction of replicating
1132 viral ancestors. Proceedings of the National Academy of Sciences of the United States of America.
1133 2019;116(51):25891-25899. Epub 2019/11/27. doi: 10.1073/pnas.1910334116.

128. Tamura K, Stecher G, Peterson D, Filipski A, Kumar S. MEGA6: Molecular Evolutionary Genetics Analysis version 6.0. Molecular Biology and Evolution. 2013;30(12):2725-2729. Epub 2013/10/16. doi: 10.1093/molbev/mst197.

129. Pettersen EF, Goddard TD, Huang CC, Couch GS, Greenblatt DM, Meng EC, et al. UCSF Chimera--a visualization system for exploratory research and analysis. Journal of Computatinal Chemistry. 2004;25(13):1605-1612. doi: 10.1002/jcc.20084.

130. Shapovalov MV, Dunbrack RL. A smoothed backbone-dependent rotamer library for proteins derived from adaptive kernel density estimates and regressions. Structure. 2011;19(6):844-858. doi: 10.1016/j.str.2011.03.019.

Figure captions

Fig 1. The location of previously reported Env mutations that overcome blocks to virus replication (Van Duyne et al., PNAS, 2019 [48]) (A) Schematic of the HIV-1 Env-coding region with the position of mutations indicated using NL4-3 (and HXB2, in parentheses) numbering. Labeled domains are defined as follows: C1–C5, constant region 1–5; V1–V5, variable region 1–5; FP, fusion peptide; HR1/HR2, heptad repeat 1/2; DSL, disulfide loop; MPER, membrane proximal external region; TM, transmembrane; CT, cytoplasmic tail. (B) A prefusion Env structure of subtype B JR-FL SOSIP.664 (PDB accession number 5FYK [96]) with the position of the Env mutations highlighted. Most of gp120 is shown in white, with gp120 V1/V2 and V3 loops colored in light yellow and light green, respectively. gp41 is colored in tan. Y61, P81, A539 and A556 are highlighted in green, yellow, red and blue, respectively. Structural model was generated using UCSF Chimera software [129].

Fig 2. Replication kinetics of Env-A539V in the presence of INSTIs, NRTI, NNRTI, PI, ALLINI and Ent-Is. The SupT1 T-cell line was transfected with WT or Env-A539V proviral clones in the absence or in the presence of indicated concentrations of ARVs. (A and B) INSTIs, (C and D) NNRTI and NRTI, (E) PI, (F) ALLINI, and (G and H) Ent-Is. Virus replication kinetics were monitored by measuring RT activity at the indicated time points. Data are representative of at least two independent experiments. (I)

The SupT1 T-cell line was transfected with WT or Env-A539V proviral clones in the absence or in the presence of serial dilutions (0.01 – 3,000 nM) of ARVs. IC_{50} values were calculated based on RT levels at the peak of virus replication. Fold changes in IC_{50} were calculated compared to WT. Data from at least two independent experiments are shown as means ± SE. *p*-values < 0.001 (***), < 0.01 (**), < 0.05 (*) by unpaired *t*-test. The EFV and NFV data are shown on a separate bar graph to avoid compression of the y-axis.

Fig 3. Cell-free infectivity of Env-A539V in the presence or absence of ARVs. (A) RT-normalized virus stocks produced from HeLa cells were used to infect TZM-bl cells. Luciferase activity was measured at 48 hrs post-infection. Infectivity of WT NL4-3 is normalized to 1.0. (B – I) TZM-bl cells were exposed to 100 $TCID_{50}$ of WT or Env-A539V virus in the presence of varying concentrations (from 0.003 – 3,000 nM) of ARVs and incubated for 48 hrs. For NFV and BI-224436, 293T cells were transfected with the indicated proviral clones in the presence of the inhibitors. At 48 hrs post-transfection, the supernatants were used to infect TZM-bl cells. Data from at least three independent experiments are shown as mean ± SE.

Fig 4. Effect of Env-A539V and RT-Y188L mutations on susceptibility to EFV. (A) The SupT1 T-cell line was transfected with the indicated proviral clones in the absence or presence of 1,000 nM EFV. Virus replication kinetics were monitored by measuring RT activity at the indicated time points. Data are representative of three independent experiments. (B) SupT1 T cells were transfected with the indicated proviral clones in the absence or presence of serial dilutions of EFV (0.03 – 1,000 nM). The dose-dependent inhibition curve was determined based on RT values at the peak of multi-cycle spreading virus replication. (C) TZM-bl cells were exposed to 100 $TCID_{50}$ of the indicated viruses in the absence or presence of serial dilutions of EFV (0.1 – 10,000 nM). Luciferase activity was measured at 48 hrs post-infection. (D) IC_{50} values for EFV in multi-cycle spreading and cell-free infection based on the data in

Fig. 4B and C. Data from at least three independent experiments are shown as means ± SE. *p*-values < 0.001 (***), < 0.01 (**), < 0.05 (*) by unpaired *t*-test.

Fig 5. Effect of Env mutations on sCD4-induced and time-dependent gp120 shedding. (A and B) Concentrated viruses were incubated with sCD4 at the indicated concentrations at 37°C for 0 or 2 hrs. Incubated viruses were subsequently purified through a 20% sucrose cushion, and viral proteins were detected by western blotting. A representative gel for the sCD4-induced gp120 shedding assay is shown in A. The ratio of gp120 to p24 was quantified and plotted in B. Data from at least two independent experiments are shown as mean ± SE. (C) TZM-bl cells were exposed to 100 $TCID_{50}$ of the indicated viruses incubated with sCD4 prior to infection for 0 or 2 hrs. Luciferase activity was measured at 48 hrs post-infection. Data from three independent experiments are shown as mean ± SE. *p*-values < 0.001 (***), < 0.01 (**), < 0.05 (*) by unpaired *t*-test, with asterisks for 0 hr or 2 hrs incubation time points indicated in black or gray, respectively. (D and E) Concentrated viruses were incubated at 37°C for the indicated times. Incubated viruses were subsequently purified through a 20% sucrose cushion, and viral proteins were detected by western blotting. A representative gel for the time-dependent gp120 shedding assay is shown in D. The ratio of gp120 to p24 was quantified and plotted in E. Data from at least three independent experiments are shown as mean ± SE. *p*-values < 0.001 (***), < 0.01 (**), < 0.05 (*) by unpaired *t*-test.

Fig 6. The sensitivity or binding of Env-A539V to NAbs recognizing different Env conformations, anti-CD4 Ab and co-receptor antagonist. TZM-bl cells were exposed to 100 $TCID_{50}$ of WT NL4-3 or Env-A539V viruses in the presence of varying concentrations of NAbs (A - J), anti-CD4 Ab (K) and CXCR4 antagonist (L); luciferase activity was measured at 48 hrs post-infection. Data from three independent experiments are shown as mean ± SE. 293T cells transfected with the GFP-encoding reporter clone pBR43IeG expressing WT NL4-3 Env or the Env-A539V mutant were preincubated with 17b (M), 10E8 (N), PG16 (O) or PGT145 (P) at 4°C for 1 hr. KFS is an Env-defective mutant. The cells were

1213 washed, and APC-conjugated anti-human IgG was used to detect bound Ab. APC signals were
1214 normalized by GFP signal to calculate the Ab binding efficiency. Data are shown as mean ± SE from
1215 three independent experiments. *p*-values < 0.001 (***), < 0.01 (**), < 0.05 (*) by unpaired *t*-test or one-
1216 way ANOVA and Tukey's multiple comparison test.
1217
1218 **Fig 7. Selection for DTG resistance with the CCR5-tropic NL(AD8) strain.** (A) The SupT1huR5 T-
1219 cell line was transfected with pNL(AD8) in the absence or presence of 6.0 nM DTG. At the time point
1220 indicated by the arrow, DNA was extracted from the DTG-treated culture and the IN- and Env-coding
1221 regions were sequenced, leading to the identification of the Env-N654K mutation. (B) A prefusion Env
1222 structure of subtype B JR-FL SOSIP.664 (PDB accession number is 5FYK [96]), highlighting the
1223 location of Env mutations selected in the context of NL4-3 [48] and the Env-N654K mutation selected in
1224 NL(AD8). Env amino acid positions are indicated using the NL4-3 numbering. Most of gp120 is shown
1225 in white, with gp120 V1/V2 and V3 loops colored in light yellow and light green, respectively. Env-Y61,
1226 P81, and A556 are highlighted in cyan; Env-A539 and N654 are highlighted in red and purple,
1227 respectively. The structural model was generated using the UCSF Chimera software. (C) The SupT1huR5
1228 T-cell line was transfected with WT or mutant pNL(AD8) in the absence or presence of 300 or 0.3 nM
1229 DTG. Replication kinetics were monitored by measuring RT activity at the indicated time points. Data
1230 are representative of at least three independent experiments. (D) The SupT1huR5 T-cell line was
1231 transfected with WT or mutant pNL(AD8) in the absence or presence of a serial dilution of DTG (1,000
1232 nM- 0.03 nM). DTG IC_{50} values were calculated based on RT values at the peak of virus replication.
1233 Fold changes in IC_{50} relative to WT are indicated. Data from at least three independent experiments are
1234 shown as means ± SE. *p*-values < 0.001 (***), < 0.01 (**), < 0.05 (*) by unpaired *t*-test. (E) RT-
1235 normalized virus stocks produced from HeLa cells were used to infect TZM-bl cells. Luciferase activity
1236 was measured at 48 hrs post-infection. (F) TZM-bl cells were exposed to 100 $TCID_{50}$ of the indicated
1237 viruses in the presence of various concentrations of DTG and luciferase activity was measured at 48 hrs

post-infection. Data are normalized to WT and are shown as means ± SE from at least three independent experiments. *p*-values < 0.001 (***), < 0.01 (**), < 0.05 (*) by unpaired *t*-test.

Fig 8. The sensitivity of NL(AD8) Env-N654K to NAbs recognizing different Env conformations, anti-CD4 Ab, and entry inhibitors. TZM-bl cells were infected with 100 $TCID_{50}$ of the indicated viruses in the presence of various concentrations of NAbs (A- G), sCD4 (H), anti-CD4 Ab SIM.4 (I) and entry inhibitors (J – L). Luciferase activity was measured at 48 hrs post-infection. Data from at least three independent experiments are shown as means ± SE. *p*-values < 0.001 (***), < 0.01 (**), < 0.05 (*) by unpaired *t*-test. The asterisks for 0 hr or 2 hrs incubation with sCD4 (panel H) are indicated as black or gray, respectively.

Fig 9. Frequency of observed mutations in gp120 C1 domain and gp41 ectodomain in patient-derived samples from the SELECT study. (A) PID A1, A3 and A5. (B) PID A4. Positions of mutations are indicated using HXB2 numbering. FP, fusion peptide; FPPR, fusion peptide proximal region; HR1/HR2, heptad repeat 1/2; DSL, disulfide loop. Mutations observed in multiple patients are shaded in yellow. Observed residues are indicated in bold. Mutations that changed conserved positions to less conserved residues are indicated with an [a]. Frequencies were determined for subtype C sequences (n = 5,923) retrieved from the Los Alamos HIV Database. Fischer's exact test was performed to determine statistical significance. *p*-values < 0.001 (***), < 0.01 (**), < 0.05 (*). ns: not significant, N.D.; not determined**.**

Supporting information

S1 Fig. Selection for DTG resistance with the subtype C, CCR5-tropic strain K3016. (A) The SupT1huR5 T-cell line was transfected with pNL(AD8) in the absence or presence of 3.0 nM DTG. At the time point indicated by the arrow, DNA was extracted from the DTG-treated culture and the IN- and

Env-coding regions were sequenced, leading to the identification of the Env-T529I mutation. (B) gp41 HR1 sequences around the K3016 Env-T529I mutation are shown aligned with the NL4-3 sequence. (C) The SupT1huR5 T-cell line was transfected with WT K3016 or the Env-T529I derivative in the absence of DTG. The supernatants collected at the indicated time points were assayed for replication kinetics by measuring RT activity. Data are representative of at three independent experiments. (D) The SupT1huR5 T-cell line was transfected with WT K3016 or the Env-T529I derivative in the absence or presence of a serial dilution of DTG (0.03 – 1,000 nM). IC_{50}s were calculated based on RT values at the peak of virus replication. Fold changes in IC_{50} relative to WT were calculated. Data from at least three independent experiments are shown as means ± SE. *p*-values < 0.001 (***), < 0.01 (**), < 0.05 (*) by unpaired *t*-test.

S2 Fig. Comparison of the sensitivity of NL4-3 and NL(AD8) to NAbs, DTG, T-20, and sCD4 in cell-free infection. TZM-bl cells were infected with 100 $TCID_{50}$ of the indicated viruses in the presence of varying concentrations of NAbs (A – F), ARVs (H and I), and sCD4 (J). sCD4 incubations were performed for 0 or 2 hrs. The data are related to Fig. 3 and 8. Data from at least three independent experiments are shown as means ± SE.

S3 Fig. Analysis of sCD4-induced and time-dependent gp120 shedding of NL(AD8) Env mutants and comparison of NL4-3 vs. NL(AD8) gp120 shedding. (A) Concentrated viruses were incubated with the indicated concentrations of sCD4 at 37°C for 2 hrs. Incubated viruses were subsequently purified through 20% sucrose cushions, and viral proteins were detected by western blotting. A representative gel is shown. (B) Viruses were incubated at 37°C for the indicated times. Incubated viruses were subsequently purified through 20% sucrose cushions, and viral proteins were detected by western blotting. A representative gel is shown. Quantification of sCD4-induced (C) and time-dependent (D) gp120 shedding from three independent experiments, calculated as the ratio of virion-associated gp120/p24 and shown as mean ± SE. Comparison of NL4-3 and NL(AD8) sCD4-induced (E) and time-

dependent (F) gp120 shedding. The data are related to Fig. 5 and S3. Data from at least three independent experiments are shown as mean ± SE. *p*-values < 0.001 (***), < 0.01 (**), < 0.05 (*), by unpaired *t*-test.

S4 Fig. Structural models of NL4-3 Env-Y61H, A539V and A556T mutations. Unliganded Env structure (PDB: 5FYK [96]) in shown at the top left. gp120 and gp41 of protomer 1 are indicated in white and light blue, respectively. Other protomers are indicated in gray. Residues Y61, A539 and A556 are highlighted in green, red and blue, respectively. *In silico* mutagenesis and analysis of possible contacts were performed with UCSF Chimera software [129, 130]. Residues that contact the mutated residues are indicated in magenta. Env amino acid positions are indicated using the NL4-3 numbering. Possible contacts are highlighted as yellow lines.

S5 Fig. Structural models of the NL4-3 Env-P81S mutant. (A) Unliganded Env structure (PDB: 5FYK [96]) (B) CD4-bound Env structure (PDB: 5VN3 [95]). gp120 and gp41 of protomer 1 are indicated in white and light blue, respectively. Other protomers are indicated in gray. Residue P81 is highlighted in orange. *In silico* mutagenesis and analysis of possible contacts were performed by UCSF Chimera software [129, 130]. Residues that contact the mutated residues are indicated in magenta. Env amino acid positions are indicated using the NL4-3 numbering. Possible contacts are highlighted as yellow lines.

Fig 1

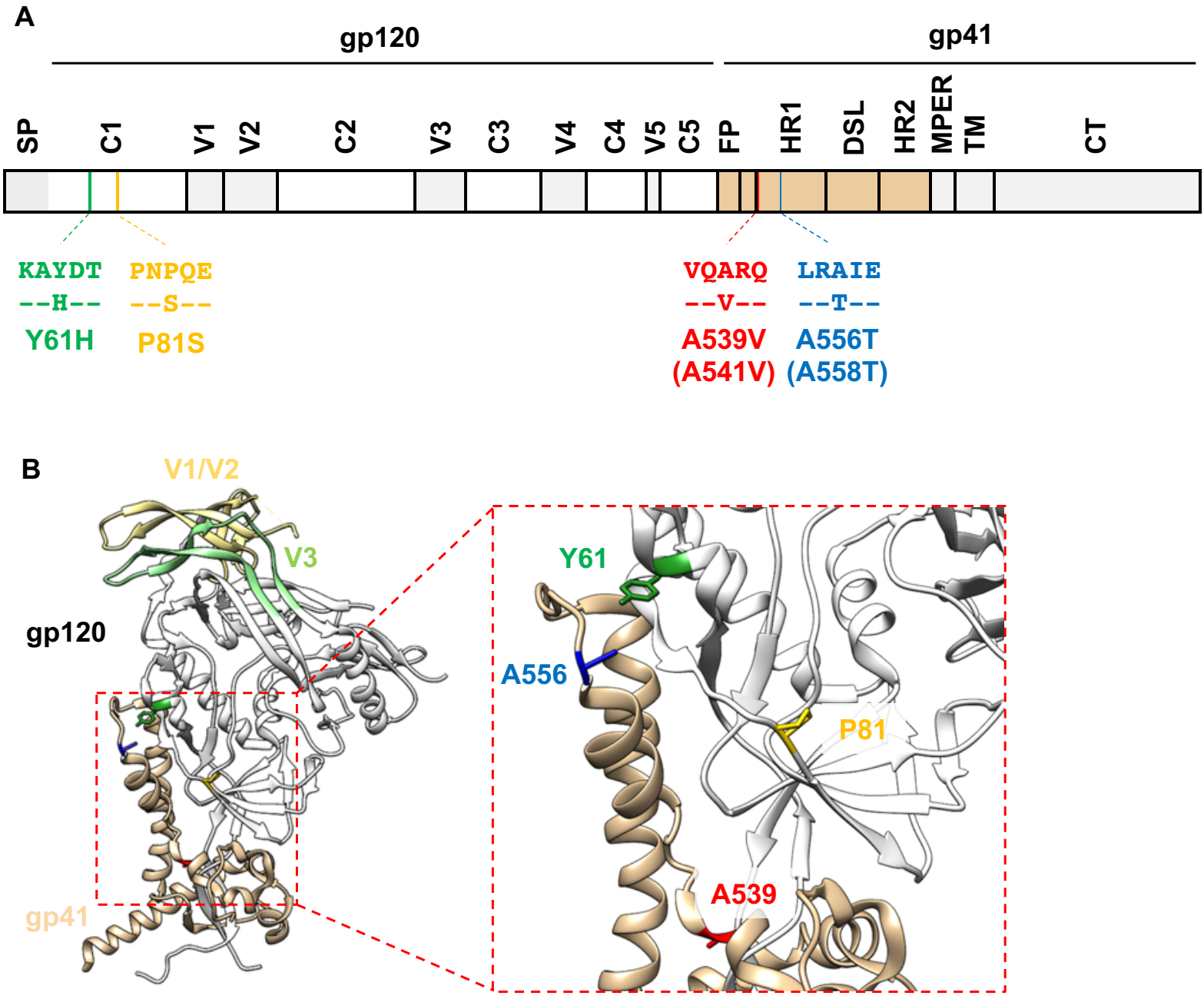
A
gp120
gp41
SP
C1
V1
V2
C2
V3
C3
V4
C4
V5
C5
FP
HR1
DSL
HR2
MPER
TM
CT
KAYDT
--H--
Y61H
PNPQE
--S--
P81S
VQARQ
--V--
A539V
(A541V)
LRAIE
--T--
A556T
(A558T)
B
V1/V2
V3
gp120
gp41
Y61
A556
P81
A539

Fig 2

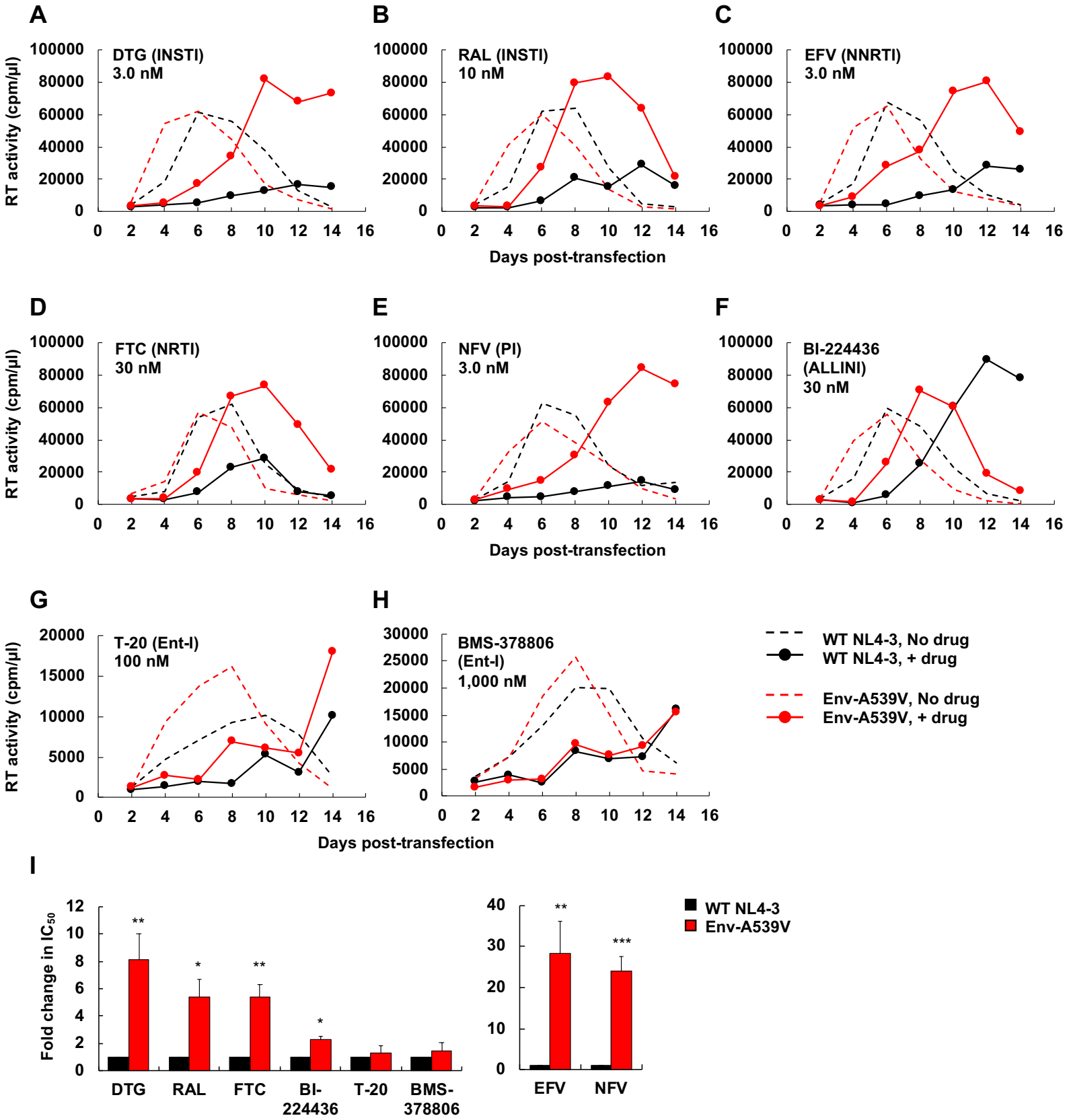
A
DTG (INSTI)
3.0 nM
B
RAL (INSTI)
10 nM
C
EFV (NNRTI)
3.0 nM
D
FTC (NRTI)
30 nM
E
NFV (PI)
3.0 nM
F
BI-224436
(ALLINI)
30 nM
G
T-20 (Ent-I)
100 nM
H
BMS-378806
(Ent-I)
1,000 nM
RT activity (cpm/µl)
Days post-transfection
WT NL4-3, No drug
WT NL4-3, + drug
Env-A539V, No drug
Env-A539V, + drug
I
Fold change in IC50
DTG
RAL
FTC
BI-224436
T-20
BMS-378806
EFV
NFV
WT NL4-3
Env-A539V

Fig 3

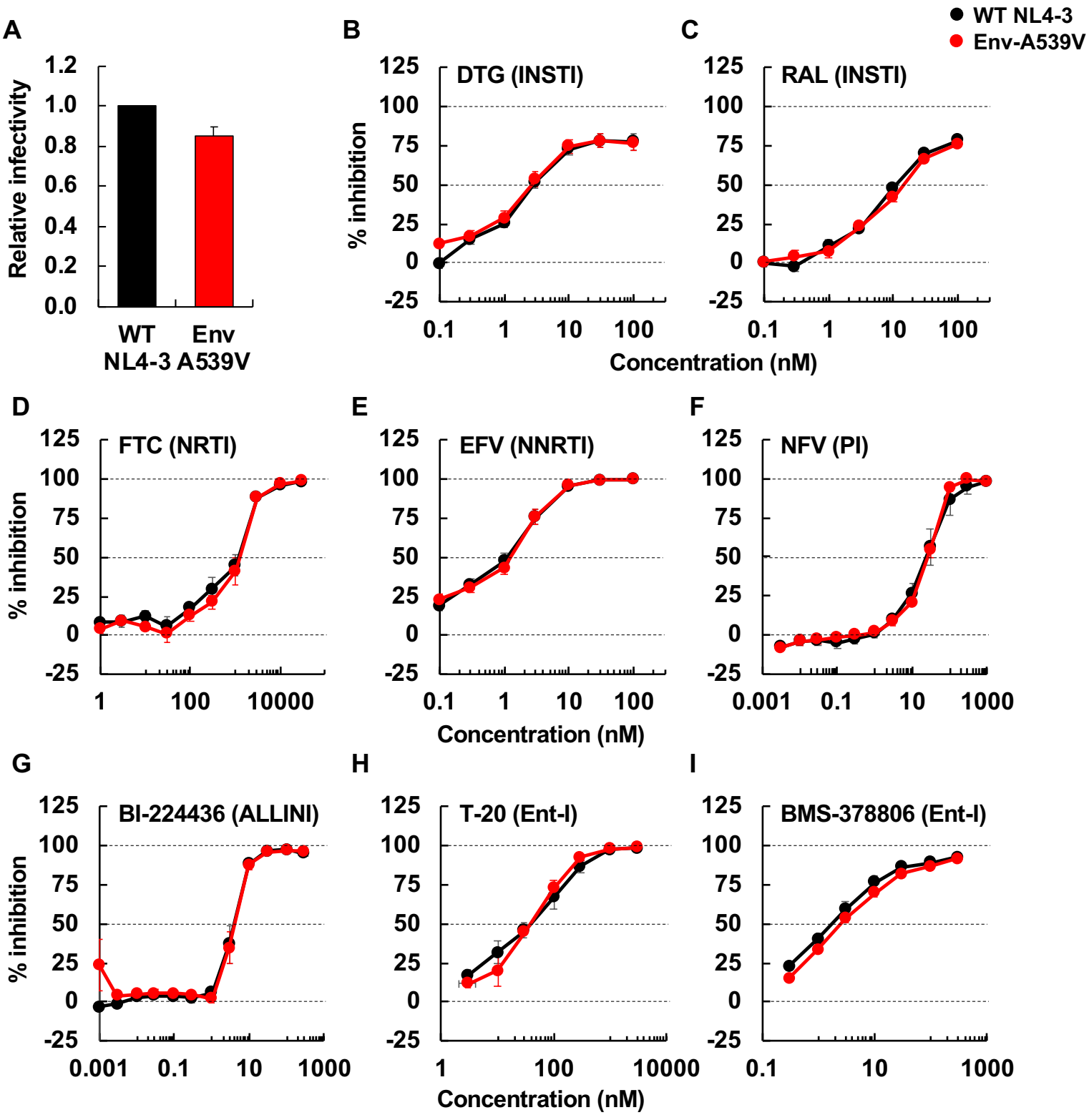
A
Relative infectivity
1.2
1.0
0.8
0.6
0.4
0.2
0.0
WT NL4-3
Env A539V
B
DTG (INSTI)
% inhibition
125
100
75
50
25
0
-25
0.1
1
10
100
C
RAL (INSTI)
Concentration (nM)
WT NL4-3
Env-A539V
D
FTC (NRTI)
% inhibition
1
100
10000
E
EFV (NNRTI)
Concentration (nM)
F
NFV (PI)
0.001
0.1
10
1000
G
BI-224436 (ALLINI)
% inhibition
H
T-20 (Ent-I)
Concentration (nM)
I
BMS-378806 (Ent-I)

Fig 4

A

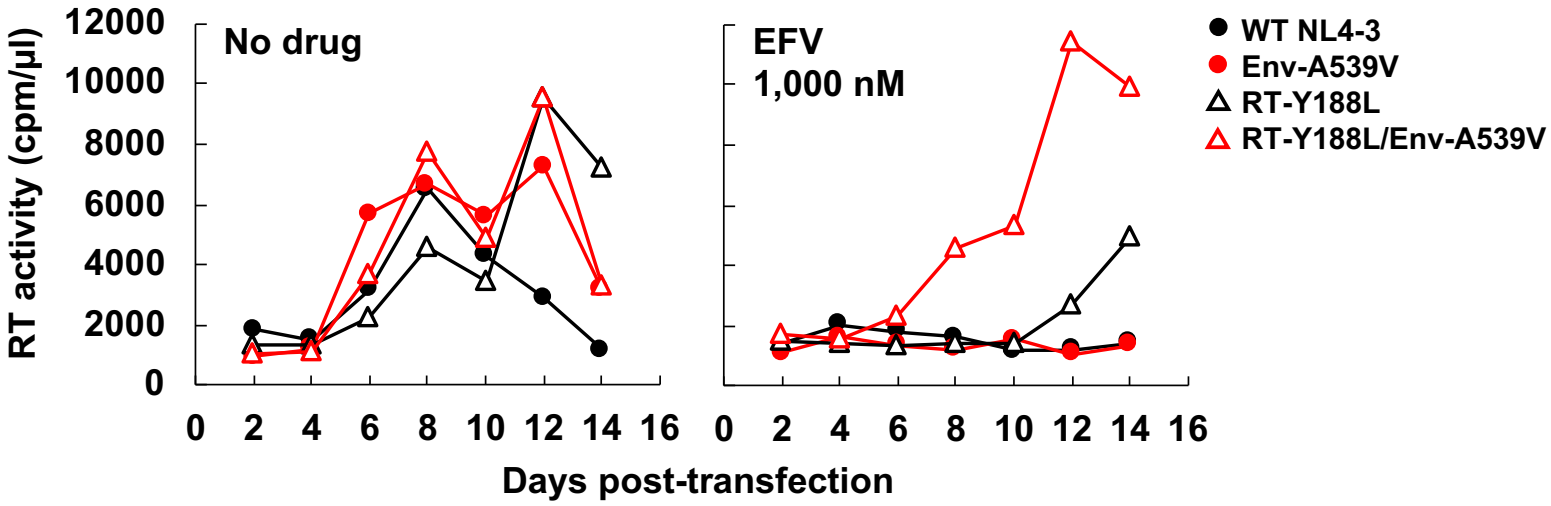

B

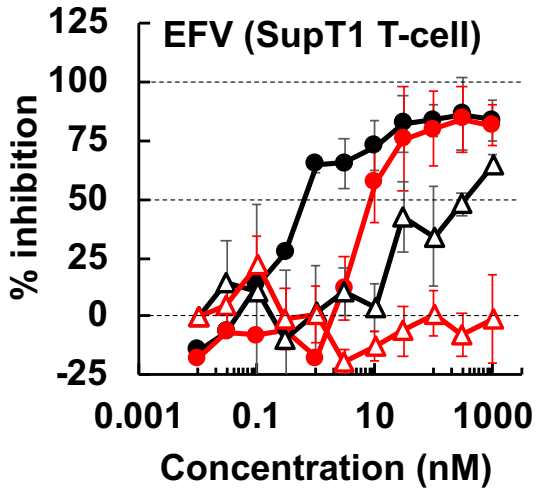

C

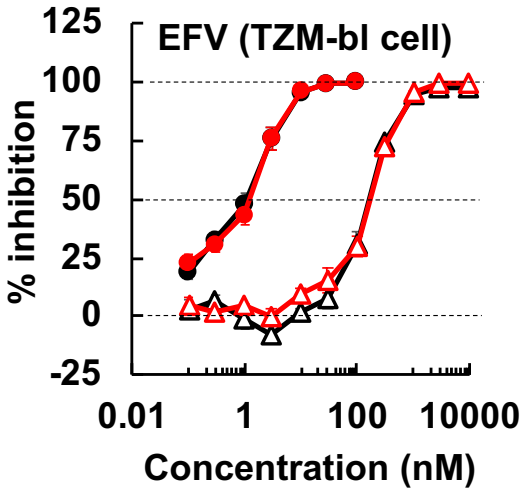

D

Viruses	IC_{50} (nM, mean ± SE)	
	Spreading	Cell-free
WT NL4-3	0.41 ± 0.13	1.2 ± 0.31
Env-A539V	18 ± 7.2	1.4 ± 0.27
RT-Y188L	388 ± 72	126 ± 10
RT-Y188L/Env-A539V	> 1,000	136 ± 5.9

Fig 5

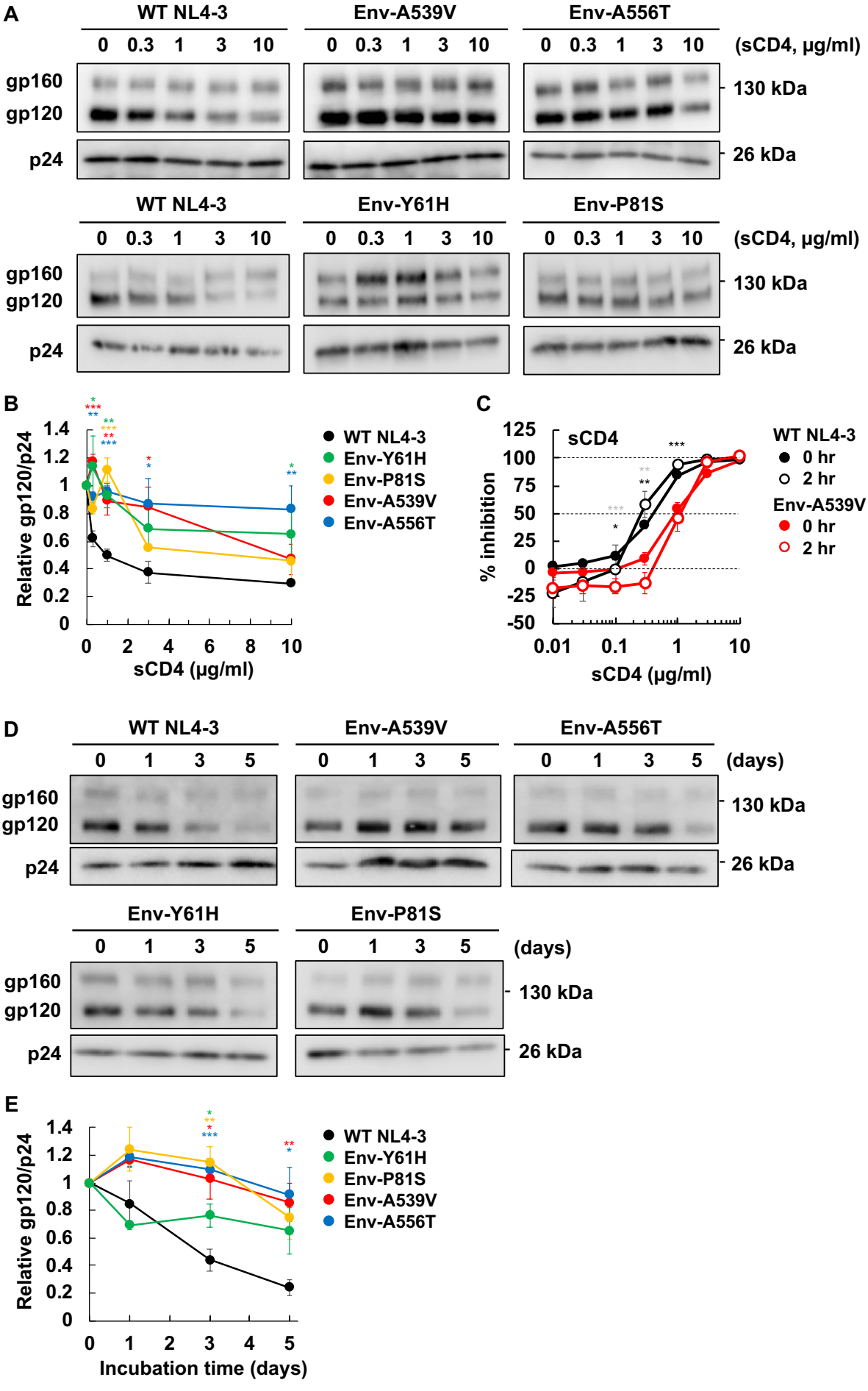
A
WT NL4-3
Env-A539V
Env-A556T
0 0.3 1 3 10
(sCD4, μg/ml)
gp160
gp120
p24
130 kDa
26 kDa
WT NL4-3
Env-Y61H
Env-P81S
B
Relative gp120/p24
sCD4 (μg/ml)
WT NL4-3
Env-Y61H
Env-P81S
Env-A539V
Env-A556T
C
sCD4
% inhibition
sCD4 (μg/ml)
WT NL4-3
0 hr
2 hr
Env-A539V
0 hr
2 hr
D
WT NL4-3
Env-A539V
Env-A556T
0 1 3 5
(days)
gp160
gp120
p24
130 kDa
26 kDa
Env-Y61H
Env-P81S
E
Relative gp120/p24
Incubation time (days)
WT NL4-3
Env-Y61H
Env-P81S
Env-A539V
Env-A556T

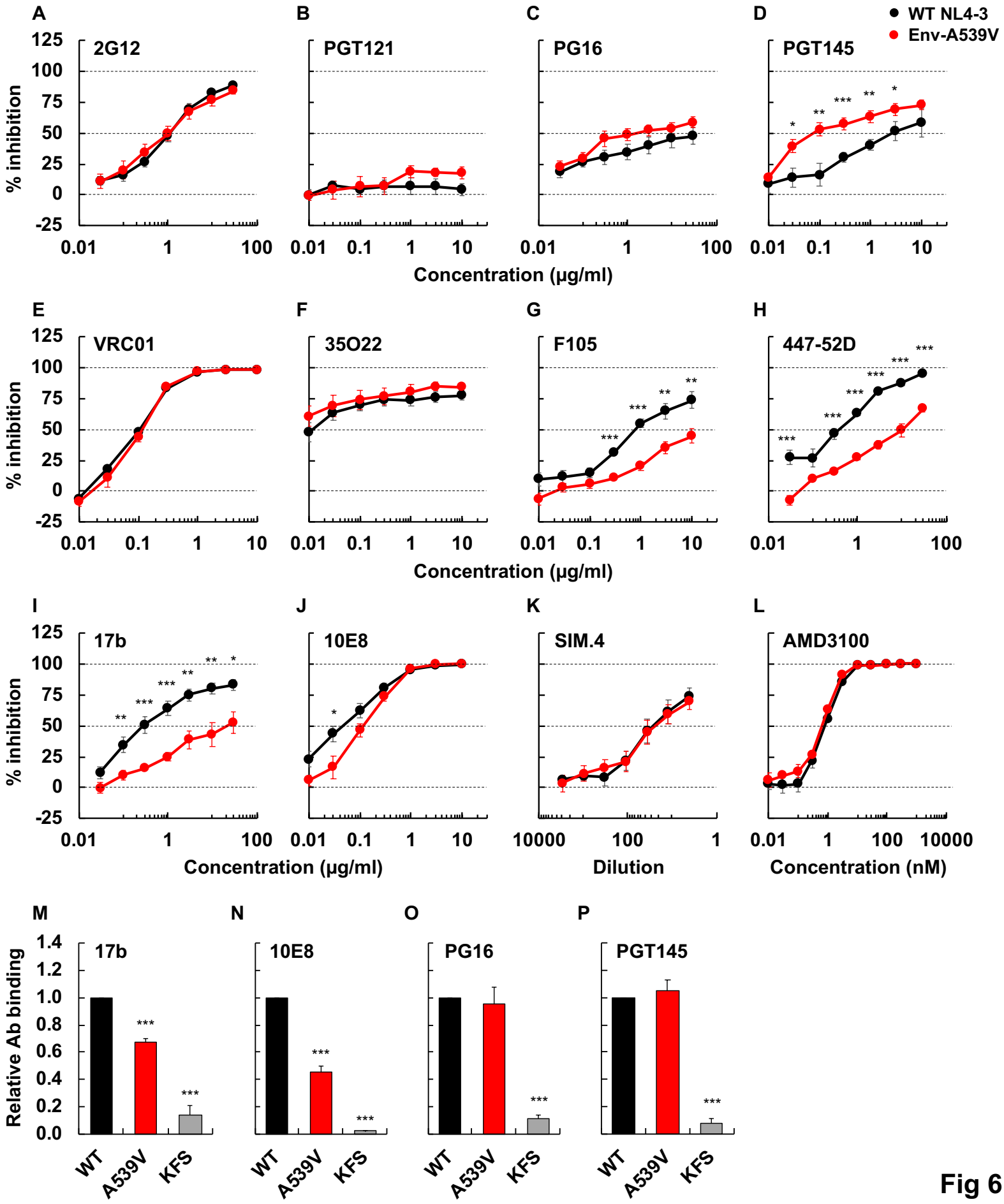
A
B
C
D
WT NL4-3
Env-A539V
2G12
PGT121
PG16
PGT145
% inhibition
Concentration (μg/ml)
E
F
G
H
VRC01
35O22
F105
447-52D
I
J
K
L
17b
10E8
SIM.4
AMD3100
Dilution
Concentration (nM)
M
N
O
P
Relative Ab binding
WT
A539V
KFS

Fig 6

Fig 7

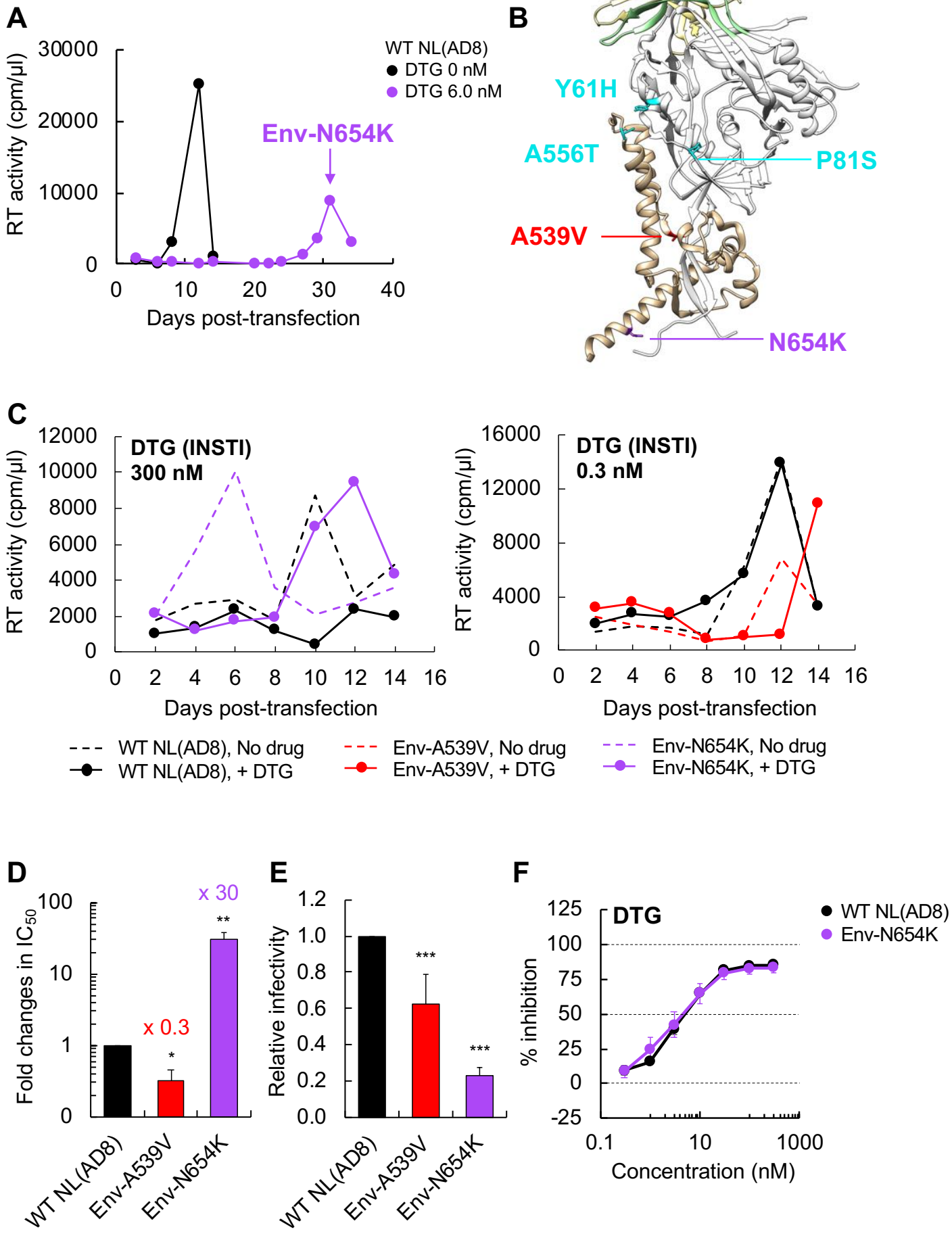
A
RT activity (cpm/μl)
30000
20000
10000
0
0
10
20
30
40
Days post-transfection
WT NL(AD8)
DTG 0 nM
DTG 6.0 nM
Env-N654K
B
Y61H
A556T
P81S
A539V
N654K
C
DTG (INSTI)
300 nM
RT activity (cpm/μl)
12000
10000
8000
6000
4000
2000
0
0
2
4
6
8
10
12
14
16
Days post-transfection
DTG (INSTI)
0.3 nM
RT activity (cpm/μl)
16000
12000
8000
4000
0
0
2
4
6
8
10
12
14
16
Days post-transfection
WT NL(AD8), No drug
WT NL(AD8), + DTG
Env-A539V, No drug
Env-A539V, + DTG
Env-N654K, No drug
Env-N654K, + DTG
D
Fold changes in IC50
100
10
1
0
x 30
**
x 0.3
*
WT NL(AD8)
Env-A539V
Env-N654K
E
Relative infectivity
1.2
1.0
0.8
0.6
0.4
0.2
0.0
***
***
WT NL(AD8)
Env-A539V
Env-N654K
F
DTG
% inhibition
125
100
75
50
25
0
-25
0.1
10
1000
Concentration (nM)
WT NL(AD8)
Env-N654K

Fig 8

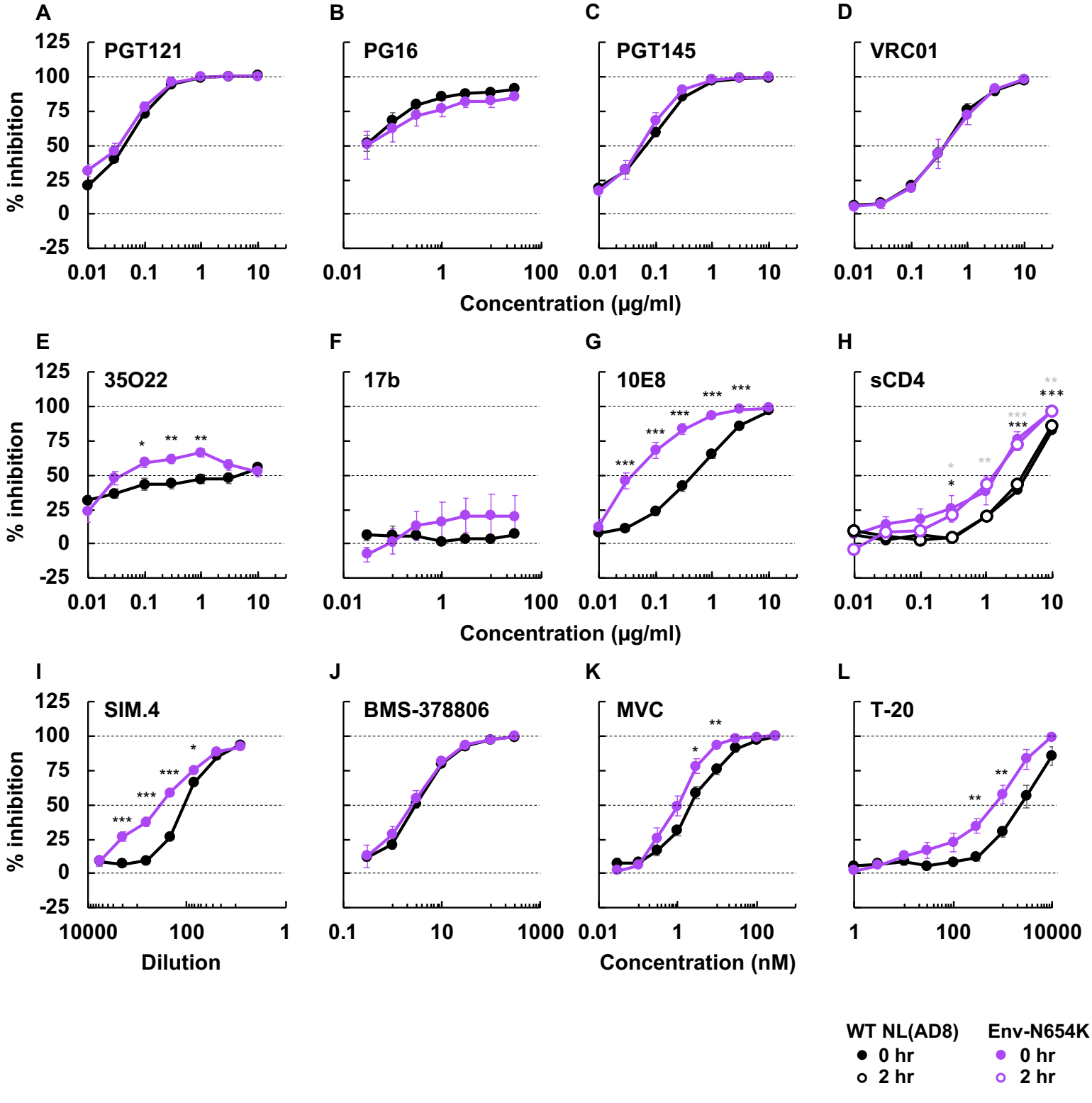
A
PGT121
B
PG16
C
PGT145
D
VRC01
E
35O22
F
17b
G
10E8
H
sCD4
I
SIM.4
J
BMS-378806
K
MVC
L
T-20
% inhibition
Concentration (μg/ml)
Dilution
Concentration (nM)
WT NL(AD8)
0 hr
2 hr
Env-N654K
0 hr
2 hr

Fig 9A

Participant identifers	Mutations			Frequency (%) Pre	Early		Late		Frequency of residues (%) in subtype C Env
A1	gp120	C1	E32R[a]	4.8	0	ns	22	*	G: 51.32, V: 14.47, **E: 9.21**, K: 6.58, N: 5.26, D: 3.95, S: 2.63, **R: 2.63**, other: 3.95
			D62N[a]	0	0	ns	22	**	E: 75.53, **D: 18.54**, K: 2.34, **other: 3.58**
			D113N[a]	7.1	44	*	22	ns	**D: 96.90**, **other: 3.10**
	gp41	FP	V525A	4.5	0	ns	22	*	**A: 91.66**, **V: 3.31**, T: 3.10, other: 1.93
		HR2	N637S[a]	2.3	44	**	22	*	**N: 97.11**, **other: 2.89**
			R655K	6.8	0	ns	22	*	**K: 53.89**, Q: 21.09, **R: 10.82**, E: 7.17, N: 3.24, other: 3.79
A3	gp120	C1	V87A	38	100	*	100	*	E: 56.04, G: 21.35, K: 10.33, **A: 3.35** **V: 3.28**, D: 1.74, other: 3.91
	gp41	FP	T514G	3.6	80	**	75	**	**G: 95.63**, **other: 4.37**
			M518V	7.1	80	**	100	***	**V: 77.67**, **M: 12.54**, L: 7.99, other: 1.79
			A525V[a]	3.6	80	**	75	**	**A: 91.66**, **V: 3.31**, T: 3.10, other: 1.93
		HR1	Q581L	32	100	**	100	*	**L: 99.24**, **other: 0.76**
			V583I	3.6	80	**	75	**	**I: 78.08**, L: 14.06, **V: 5.31**, M: 2.55
		DSL	V595M	18	80	*	75	*	I: 55.20, L: 36.04, **M: 7.65**, **other: 1.10**
		HR2	K633R	32	100	**	100	*	**R: 73.19**, **K: 24.67**, other: 2.14
			M644R	3.6	60	**	75	**	**R: 50.10**, K: 14.27, Q: 7.99, N: 6.20, S: 5.31, T: 3.45, E: 3.45, G: 2.96, W: 2.48, **other: 3.79**
			E647A[a]	0	60	**	75	***	**E: 95.79**, **other: 4.21**
A5	gp41	FP	T514G	26	N.D.		95	***	**G: 95.63**, **other: 4.37**
			L518V	30	N.D.		95	***	**V: 77.67**, M: 12.54, **L: 7.99**, other: 1.79
			F523L	30	N.D.		95	***	**L: 90.55**, **F: 7.72**, other: 1.72
		HR1	A546S	30	N.D.		95	***	**S: 96.83**, **other: 3.17**
		DSL	L602R[a]	26	N.D.		95	***	**L: 89.94**, I: 3.86, V: 1.65, **other: 4.55**
			G624E	30	N.D.		95	***	D: 46.55, N: 20.07, **E: 14.90**, **G: 10.69**, K: 3.38, other: 4.41
		HR2	A654T	33	N.D.		95	***	E: 97.59, **other: 2.41**

Fig 9B

Participant identifers	Mutations			Frequency (%)					Frequency of residues (%) in subtype C Env
				Pre	Early		Late		
A4	gp120	C1	N57D	17	100	***	100	***	**D: 93.52**, **N: 3.79**, other: 2.69
			G60A	0	100	***	100	***	**A: 89.32**, **G: 7.10**, other: 3.58
			K63Q[a]	0	100	***	100	***	**K: 50.17**, R: 28.12, T: 15.02, **Q: 1.86**, other: 4.82
			I68V	0	100	***	100	***	**V: 88.97**, **I: 9.93**, other: 1.10
			D/N78S[a]	0	100	***	100	***	**D: 98.14**, **other: 1.86**
			I/L84M	33	100	*	100	*	**M: 35.98**, **I: 35.08, L: 21.85**, V: 5.03, other: 2.07
			M/K/I85V	26	100	*	100	*	**V: 65.33**, F: 8.20, E: 4.20, **I: 4.14**, L: 3.79, D: 2.34, A: 2.07, **K: 1.93**, P: 1.31, N: 1.17, R: 1.10, **other: 4.41**
			G/K87E	32	100	*	100	*	**E: 56.04**, **G: 21.35**, **K: 10.33**, A: 3.35, V: 3.28, D: 1.74, other: 3.91
			H105Q[a]	3.3	100	***	100	***	**H: 95.31**, **other: 4.69**
			T130N	3.3	100	***	100	***	**N: 62.76**, K: 7.24, E: 6.90, T: 4.76, H: 4.48, D: 4.21, R: 3.31, S: 2.55, **other: 3.79**
	gp41	FP	L515I	35	48	ns	93	***	**I: 67.72**, **L: 22.34**, M: 7.52, other: 2.41
		FPPR	L529F	18	100	***	100	***	T: 99.45, **other: 0.55**
			I535M[a]	0	41	***	93	***	**I: 79.39**, **M: 8.61**, V: 6.00, L: 5.72, other: 0.28
			A536T	35	59	ns	6.7	*	**T: 89.32**, **A: 9.24**, other: 1.45
		HR1	S553N[a]	0	40.7	***	93	***	**S: 83.87**, **N: 15.02**, other: 1.10
			R557K[a]	0	59.3	***	6.7	ns	**R: 88.35**, **K: 10.48**, other: 1.17
			A578T[a]	0	100	***	100	***	**A: 59.68**, **T: 40.25**, E: 0.07
			I583L[a]	0	100	***	100	***	**I: 78.08**, **L: 14.06**, V: 5.31, M: 2.55
		DSL	L595I	0	100	***	100	***	**I: 55.20**, **L: 36.04**, M: 7.65, other: 1.10
			K601I[a]	0	100	***	100	***	**K: 98.14**, **other: 1.86**
			P605T	0	100	***	100	***	**T: 95.24**, **other: 4.76**
			A607N[a]	0	100	***	100	***	**A: 51.96**, **N: 30.88**, T: 10.06, S: 4.20, other: 2.89
			S612D[a]	0	100	***	100	***	**S: 75.40**, T: 6.20, A: 4.55, **N: 4.00**, I: 2.00, D: 1.93, V: 1.24, other: 4.69
			R617K	0	100	***	100	***	**K: 84.13**, **R: 14.63**, other: 1.24
			E620K[a]	0	100	***	100	***	**E: 22.83**, T: 19.79, D: 17.17, N: 7.52, **K: 7.52**, S: 6.97, A: 6.07, G: 4.97, Q: 2.97, other: 4.21
			Y621E	0	100	***	100	***	D: 53.27, **E: 34.67**, **Y: 3.58**, A: 2.55, Q: 2.14, other: 3.79
			G624D	0	100	***	100	***	**D: 46.55**, N: 20.07, E: 14.90, **G: 10.69**, K: 3.38, other: 4.41
			N625K[a]	0	100	***	100	***	**N: 96.35**, **other: 3.65**
		HR2	R633K[a]	0	100	***	100	***	**R: 73.19**, **K: 24.67**, other: 2.14
			D636S	0	100	***	100	***	**S: 53.55**, N: 31.36, **D: 11.58**, other: 3.51
			T641I[a]	27	0	**	0	**	**T: 72.78**, **I: 21.23**, L: 1.65, other: 4.34
			N644G	0	100	***	100	***	R: 50.10, K: 14.27, Q: 7.99, **N: 6.20**, S: 5.31, T: 3.45, E: 3.45, **G: 2.96**, W: 2.48, other: 3.79
			I648E	0	100	***	100	***	**E: 38.83**, D: 38.69, V: 9.10, K: 5.38, **I: 3.31**, other: 4.69
			N651A/T[a]	0	100	***	100	***	**N: 54.72**, I: 16.26, **T: 12.61**, S: 11.30, K: 0.76, **other: 4.34**
			K655N[a]	0	100	***	100	***	**K: 53.89**, Q: 21.09, R: 10.82, E: 7.17, **N: 3.24**, other: 3.79
			E658K	0	100	***	100	***	**K: 81.53**, Q: 13.65, **other: 4.82**
			K662A/T	12	100	***	100	***	**A: 89.87**, E: 7.51, **other: 2.62**
			N665K	0	100	***	100	***	S: 66.09, **K: 26.46**, **N: 3.24**, other: 4.20

S1 Fig

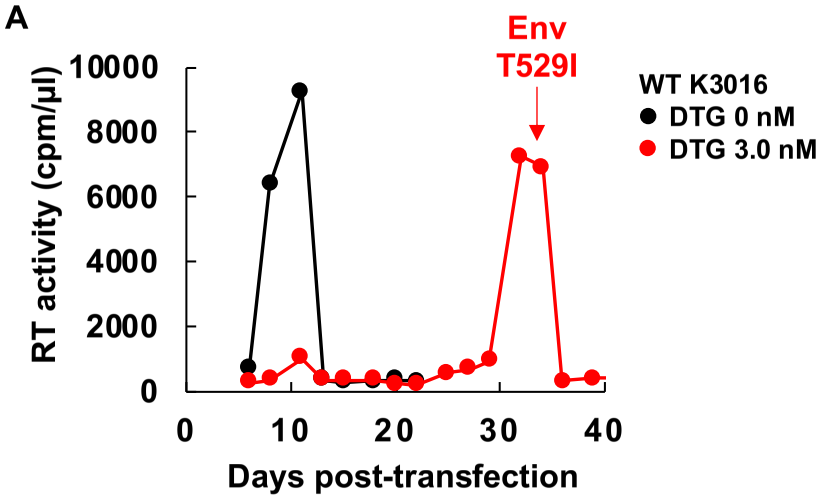

B

```
NL4-3_WT          T L T V Q A R Q L L S
NL4-3_A539V       . . . . . V . . . . .
K3016             . . . . . T . . . . .
K3016_T529I       . . . . . I . . . . .
```

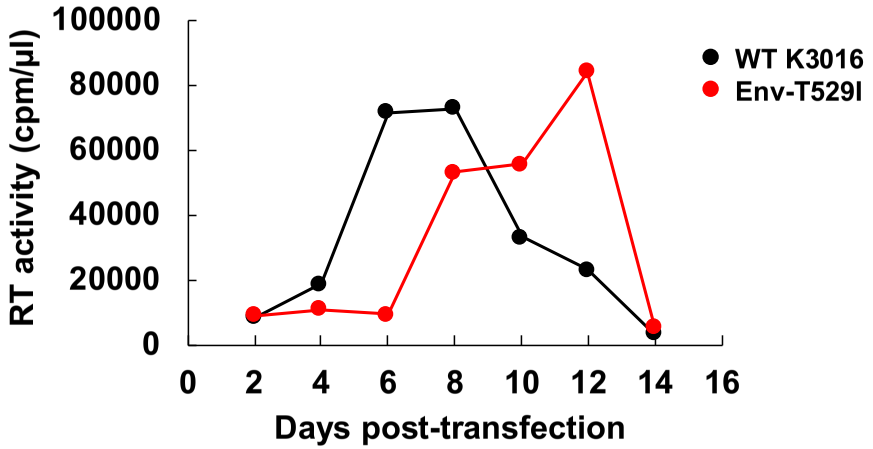

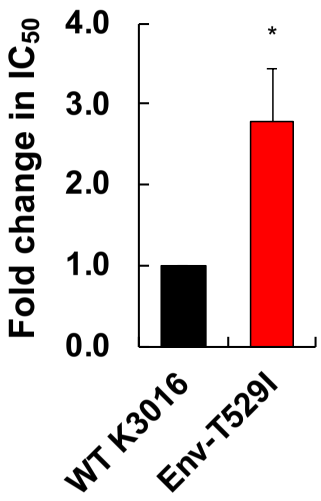

S2 Fig

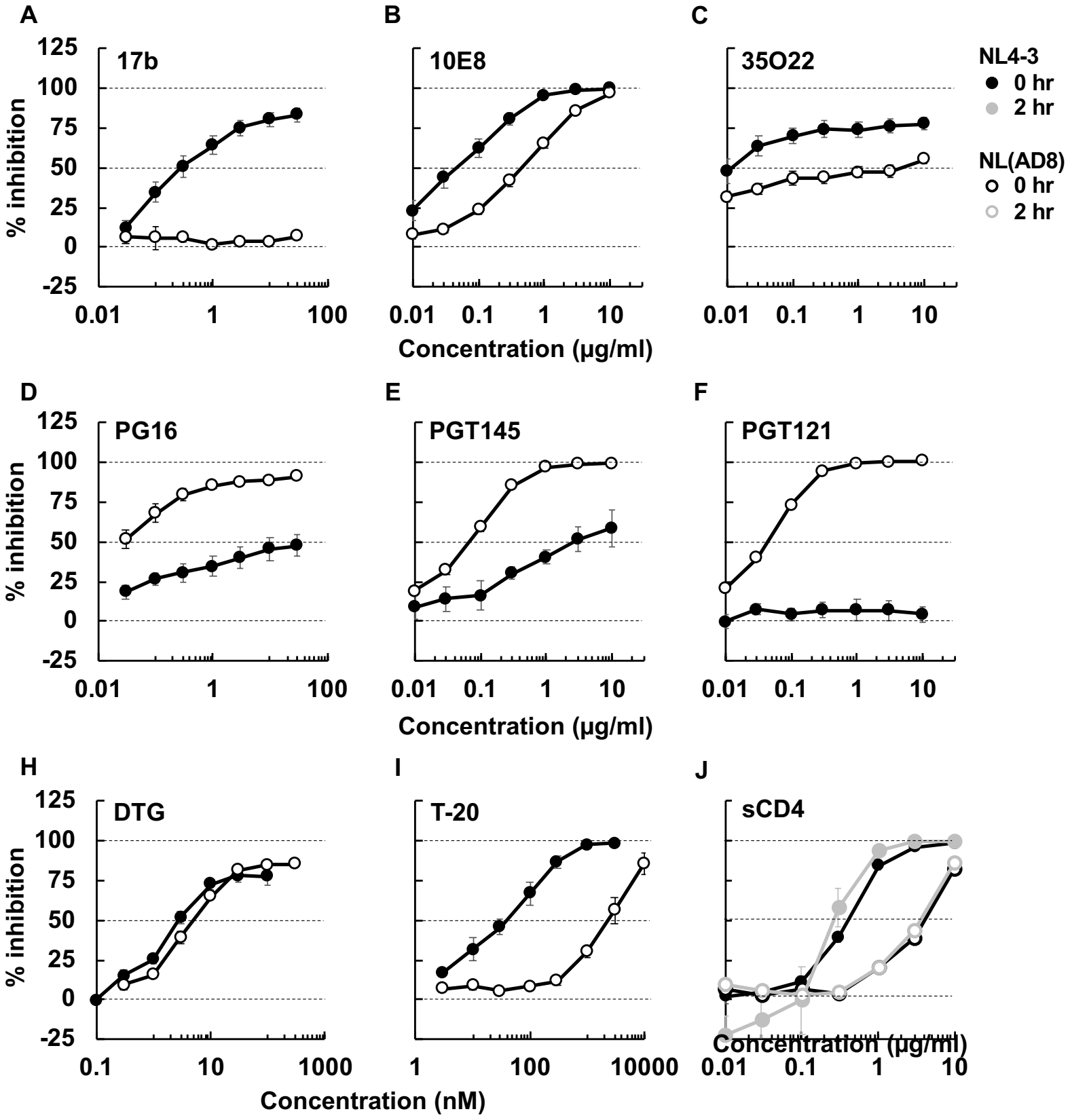
A
B
C
17b
10E8
35O22
NL4-3
0 hr
2 hr
NL(AD8)
0 hr
2 hr
% inhibition
125
100
75
50
25
0
-25
0.01
1
100
0.01
0.1
1
10
Concentration (μg/ml)
D
E
F
PG16
PGT145
PGT121
H
I
J
DTG
T-20
sCD4
0.1
10
1000
1
100
10000
Concentration (nM)
Concentration (μg/ml)

S3 Fig

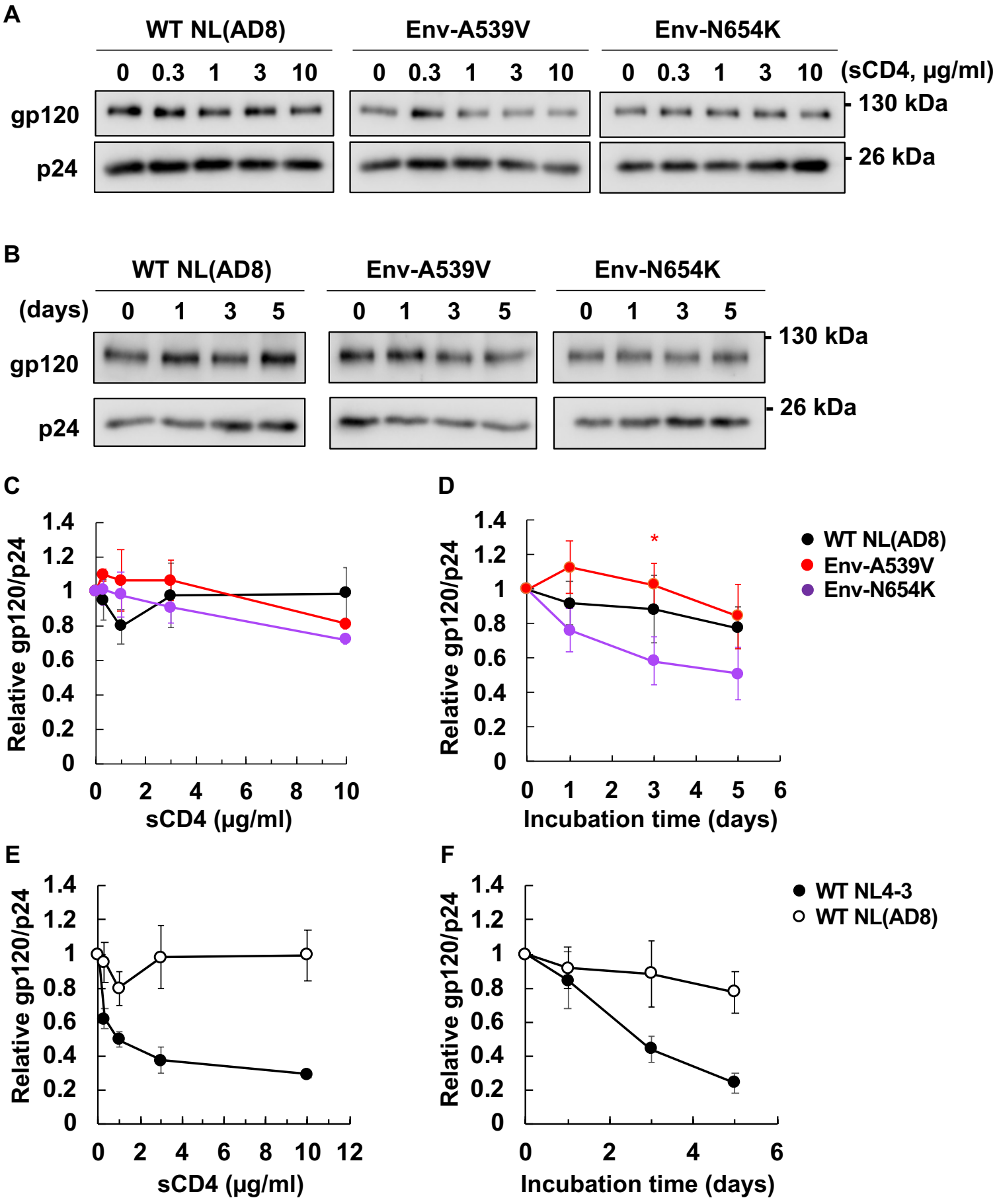
A
WT NL(AD8)
Env-A539V
Env-N654K
0 0.3 1 3 10
0 0.3 1 3 10
0 0.3 1 3 10
(sCD4, μg/ml)
gp120
p24
130 kDa
26 kDa
B
WT NL(AD8)
Env-A539V
Env-N654K
(days) 0 1 3 5
0 1 3 5
0 1 3 5
gp120
p24
130 kDa
26 kDa
C
Relative gp120/p24
sCD4 (μg/ml)
D
Relative gp120/p24
Incubation time (days)
*
WT NL(AD8)
Env-A539V
Env-N654K
E
Relative gp120/p24
sCD4 (μg/ml)
F
Relative gp120/p24
Incubation time (days)
WT NL4-3
WT NL(AD8)

S4 Fig

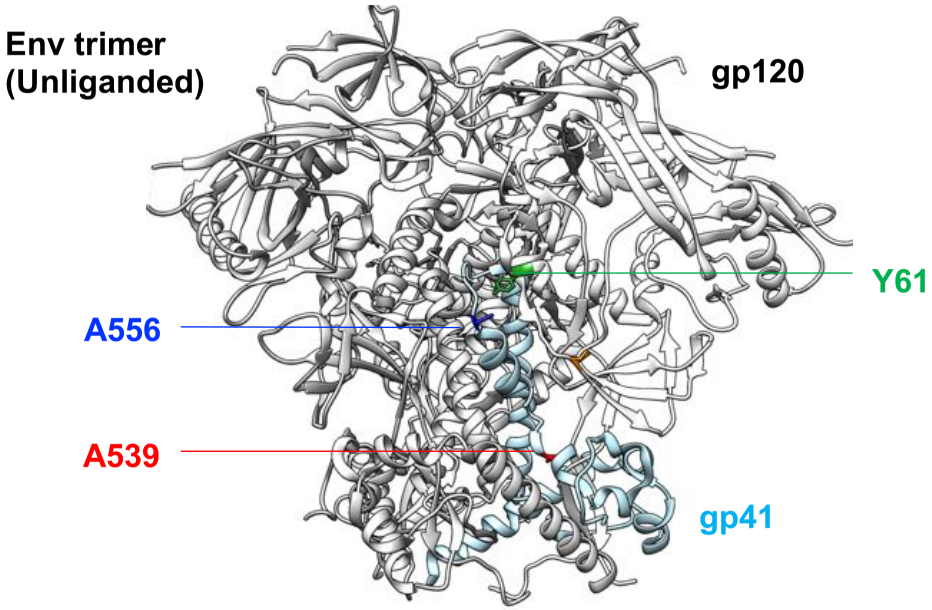
Env trimer
(Unliganded)
gp120
Y61
A556
A539
gp41

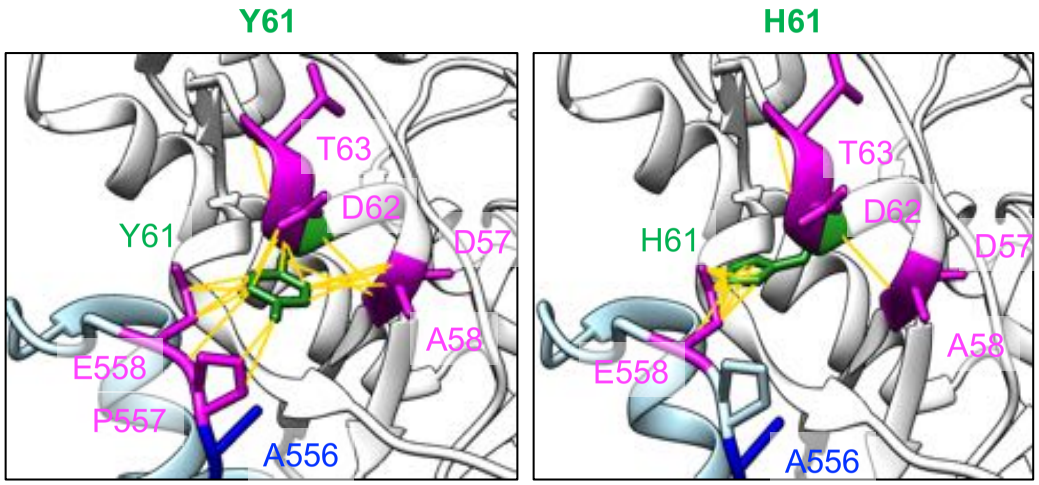
Y61
T63
D62
Y61
D57
A58
E558
P557
A556
H61
T63
D62
H61
D57
A58
E558
A556

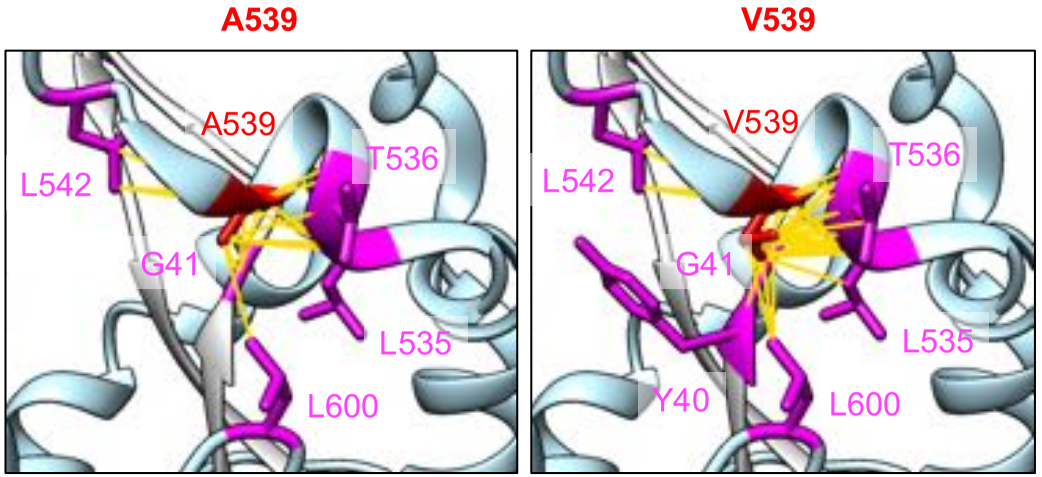
A539
A539
T536
L542
G41
L535
L600
V539
V539
T536
L542
G41
L535
Y40
L600

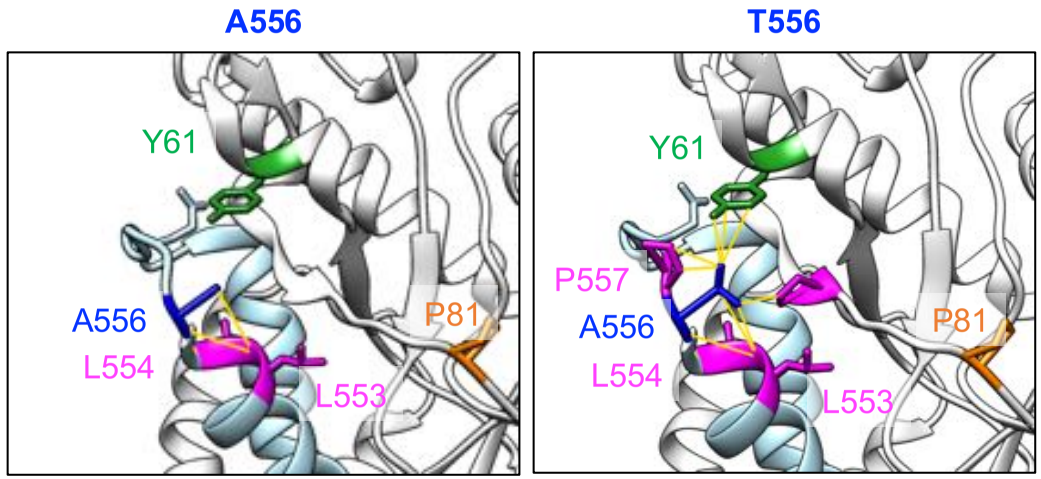
A556
Y61
A556
P81
L554
L553
T556
Y61
P557
A556
P81
L554
L553

S5 Fig

A

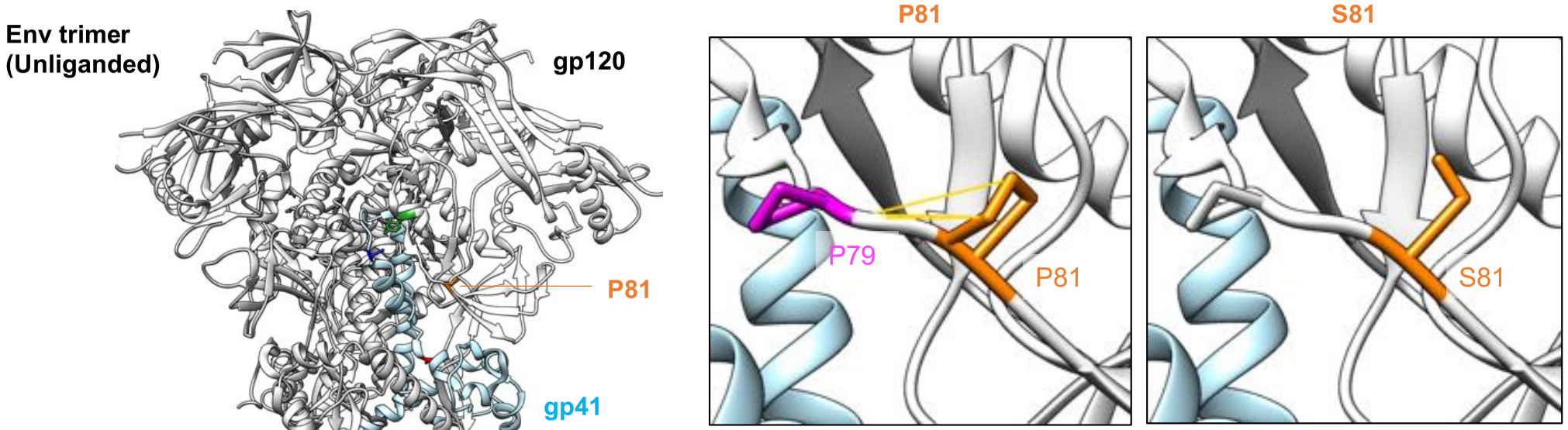
Env trimer
(Unliganded)
gp120
P81
gp41
P81
S81
P79
P81
S81

B.

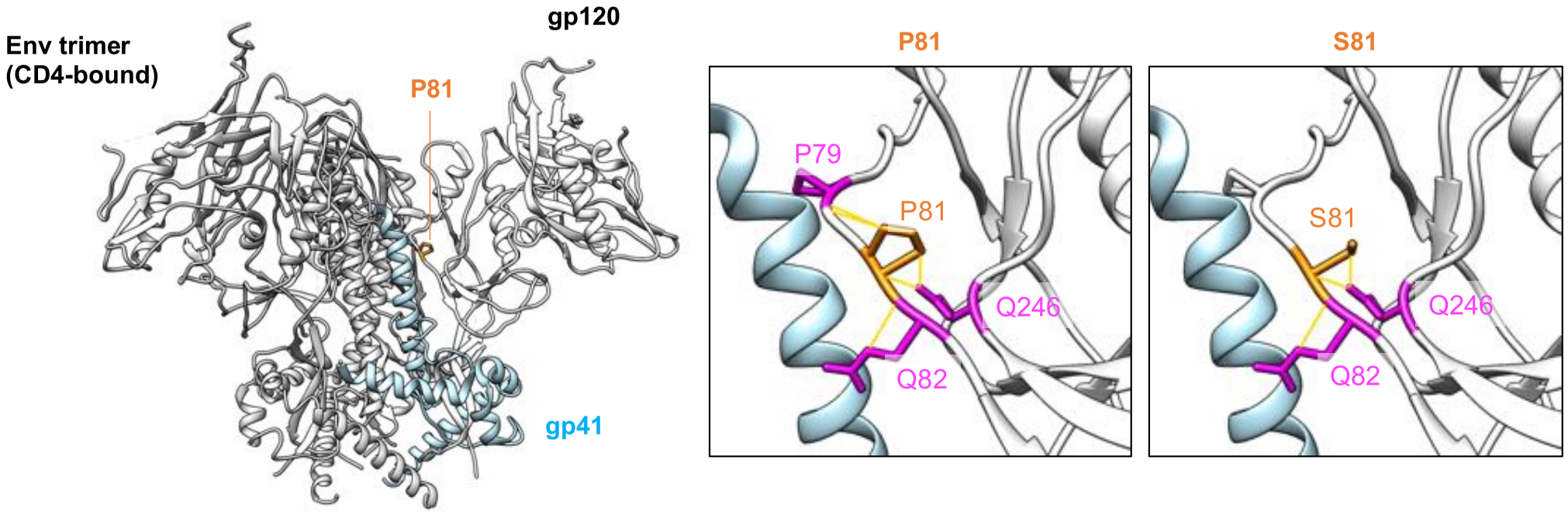
Env trimer
(CD4-bound)
gp120
P81
gp41
P81
S81
P79
P81
Q246
Q82
S81
Q246
Q82